

**ARDHI UNIVERSITY**



**OPTIMAL METHOD FOR CREATION OF CLASSICAL BOUGUER AND  
FREE-AIR GRAVITY ANOMALY DATABASE FROM ZANZIBAR 2022  
1'×1' SURFACE GRAVITY ANOMALY**

**JUMA, ABDUL-RAHIM M.**

**BSc. Geomatics**

**Dissertation**

**Ardhi University, Dar es Salaam**

**July, 2023**

OPTIMAL METHOD FOR CREATION OF CLASSICAL BOUGUER AND FREE-AIR  
GRAVITY ANOMALY DATABASE FROM ZANZIBAR 2022 1'×1' SURFACE  
GRAVITY ANOMALY

JUMA, ABDUL-RAHIM M.

22755/T.2019.

“A Dissertation, Submitted to the department of Geospatial Sciences and Technology in Partially  
Fulfillment of the Requirements for the Award of Science in Geomatics (BSc. GM) of Ardhi  
University”

## CERTIFICATION

The undersigned certify that has read and hereby recommend for the acceptance by Ardhi University, a dissertation titled “**optimal method for creation of classical bouguer and free-air gravity anomaly database from Zanzibar 2022 1'×1' surface gravity anomaly**”, in partial fulfilment of the requirements for the award of degree of Bachelor of Science in Geomatics of the Ardhi University.

Signature.....

Ms. Regina V. Peter

(Main Supervisor)

Date .....

## DECLARATION AND COPYRIGHT

I, **Abdul-rahim M. Juma**, hereby declare that the dissertation report titled “optimal method for creation of classical bouguer and free-air gravity anomaly database from Zanzibar 2022 1'×1' surface gravity anomaly” is a genuine research work carried out by me and to the best of my knowledge it has not been presented at any other university or institution of higher learning for a degree or similar award.

.....

Juma, Abdul-rahim Muhija

(Candidate)

Copyright ©1999 This dissertation is the copyright material presented under Berne convention, the copyright act of 1999 and other international and national enactments, in that belief, on intellectual property. It may not be reproduced by any means, in full or in part, except for short extracts in fair dealing; for research or private study, critical scholarly review or discourse with an acknowledgement, without the written permission of the directorate of undergraduate studies, on behalf of both the author and Ardhi University.

## **ACKNOWLEDGEMENT**

First of all, my gratitude goes to Almighty God Allah. Many praises go to him for helping me to accomplish the work. Without His grace this research would not have become a reality.

I am humbled and deeply grateful to extend my heartfelt appreciation to my extraordinary supervisor, Ms. Regina V. Peter who have left an indelible mark on my educational journey. Her unwavering dedication, tireless efforts, and passion for teaching me methodology of performing this research and her supervision during execution of this research have transformed my life in ways I could never have imagined. It was unique experience to be supervised by her.

Also, I am deeply honored to the staff members of Department of Geospatial Sciences and Technology of the Ardhi University especially the panel members Dr. Prosper E. Ulotu and Mr. Emmanuel J. Masunga for their contributions during intermediate presentation sessions which helped me in one way or another to successfully complete this research.

Without forgetting, it is with immense gratitude that I extend my heartfelt appreciation to the exceptional and my unique friends and brothers Is hak Haji Musa and Humoud Abdallah Ali, my sisters (Firdaus and Fadya) and brother Moh'd for your collaboration, intellectual exchanges, and mutual support that have created a vibrant and dynamic learning environment. To my classmates, thank you for being a part of my life and for making the educational experience truly remarkable. With deepest gratitude and appreciation, thank you for being an essential part of my educational and personal journey.

Finally, my gratitude goes to those whom their names are not reflected in this report. Their contributions will always be highly appreciated. With deepest sincerity, I extend my heartfelt thanks and eternal appreciation to each and every one of you.

## **DEDICATION**

*I dedicate this dissertation to my parents Ummul Kulthum Mohammed Haji and Muhija Juma Shehe, my brother Ismail Muhija Juma and my whole family for their love, believes, support, prayers and motivation since the beginning of my studies to the very end. All this I've done for you and I do really appreciate your presence.*

## ABSTRACT

The study of free-air and bouguer gravity anomalies plays great role in understanding the subsurface density variations, geological structures, mineral and hydrocarbon potential, crustal dynamics, and earthquake monitoring. It plays a vital role in various fields of Earth sciences and provides valuable insights into the Earth's composition, structure, and dynamic processes. This research aimed at finding the optimal method for creation of classical bouguer and free-air gravity anomaly databases by considering different approaches that lead to obtain the bouguer i.e. by varying integration radius and using LITHO1.0 crustal density model and free-air gravity anomaly databases. We focused on the computation of refine bouguer gravity anomaly databases which include bouguer, free-air and terrain corrections. The approaches that have been employed during computation of bouguer gravity anomalies were using the variable crustal density model LITHO1.0 as well as variation of inner and outer radius from the computation points during computation of the terrain correction. These variations helped to obtain different values of the terrain corrections which in turn results into different values of the bouguer gravity anomalies from which we can observe which one represent the best value and approach in computation.

The area of interest (AOI) of this research is Zanzibar and its Isles extended by 3° surrounding regions which is limited to latitude 1.75°S to 9.5°S and longitude 36°E to 43°E. Data used were 5,379-point gravity and 20 reference gravity data, ALOS v3.1-1" DEM and LITHO1.0 crustal density model. From the four attempt made during computation of the bouguer gravity anomalies, STD from the four attempts are 8.329mgal, 8.000mgal, 3.752mgal, 3.189mgal respectively and for the RMS of four attempts are 11.922mgal, 12.161mgal, 3.884mgal and 3.849mgal respectively.

These results showed that during computation of bouguer gravity anomaly, the choice of the integration radius i.e. inner radius R1 to approximately 5km and outer radius R2 to approximately 80km is referred to be optimal method for creation of classical bouguer gravity anomaly database since it came out with the smaller STD and RMS of 3.1899mgal and 3.84912mgal respectively compared to the other methods used.

**Keywords:** Bouguer gravity anomalies, free-air gravity anomalies, LITHO1.0 crustal density model, ALOS v3.1-1 DEM, Zanzibar.

## **Table of Contents**

CERTIFICATION .....	ii
DECLARATION AND COPYRIGHT.....	iii
ACKNOWLEDGEMENT .....	iv
DEDICATION .....	v
ABSTRACT.....	vi
Table of Contents .....	vii
List of Figures .....	x
List of Tables .....	xi
List of the Abbreviations .....	xii
CHAPTER ONE .....	1
INTRODUCTION .....	1
1.1 Background .....	1
1.2 Problem statement.....	3
1.3 Objectives .....	3
1.3.1 Main objectives .....	3
1.3.2 Specific objective.....	3
1.4 Significances .....	3
1.5 Output .....	4
1.6 Scope and limitations.....	4
1.7 Beneficiaries .....	4
1.8 Study area.....	4
1.9 Dissertation Outline .....	5



CHAPTER TWO .....	6
LITERATURE REVIEW .....	6
2.1 Situation of gravity in Zanzibar. ....	6
2.2 Gravity anomaly.....	9
2.3 Gravity reductions.....	11
2.3.1 Free-air reduction .....	11
2.3.2 Bouguer reduction.....	12
2.3.3 Terrain correction.....	14
2.3.4 Poincare and Prey reduction .....	15
2.4 Overview of density models .....	16
2.4.1 CRUST1.0 density model .....	16
2.4.2 Litho 1.0 crustal density model.....	17
CHAPTER THREE .....	19
METHODOLOGY .....	19
3.1 Computation of free-air gravity anomaly grid from ground gravity points.....	19
3.2 Computation of the bouguer gravity anomalies.....	21
3.2.1 Obtaining crustal density data from LITHO1.0 density model. ....	21
3.2.2 Integration radius .....	24
3.2.3 Terrain correction computation.....	25
3.3 Validation of the results .....	29
3.4 Data used.....	30
3.5 Software used.....	30
CHAPTER FOUR.....	32
RESULTS AND DISCUSSION OF THE RESULTS .....	32
4.1 Results.....	32

4.1.1 Computed normal gravity at reference ellipsoid.....	32
4.1.2 Computed free-air gravity anomalies.....	33
4.2 Bouguer gravity anomaly.....	35
4.2.1 First attempt computation of bouguer gravity anomalies .....	35
4.2.2 Second attempt computation of bouguer gravity anomalies.....	37
4.2.3 Third attempt computation of bouguer gravity anomalies.....	39
4.2.4 Fourth attempt computation of bouguer gravity anomalies. ....	41
4.3 Quality check .....	43
4.3.1 Discussion of the results .....	43
CHAPTER FIVE .....	45
CONCLUSION AND RECOMMENDATIONS .....	45
5.1 Conclusion .....	45
5.2 Recommendation .....	45
References.....	46
APPENDICES .....	48

## List of Figures

Figure 2.1: Distribution of gravity station in Zanzibar (Mussa, 2022) .....	7
Figure 2.2: Shows the location of the terrestrial ground gravity in Zanzibar (Mussa, 2022) .....	8
Figure 2.3: Aerial gravity data in Tanzania .....	9
Figure 2.4: Shows the illustration of the gravity anomaly (Vanicek, 1986) .....	10
Figure 2.5: Bouguer plate .....	13
Figure 2.6: Terrain correction ( <a href="#">Hoffman-Wellenhof &amp; Moritz, 2005</a> ) .....	14
Figure 2.7: Prey reduction ( <a href="#">Hoffman-Wellenhof &amp; Moritz, 2005</a> ) .....	15
Figure 2.8: Lateral parameterization at tessellation on the global (left) and regional (right) scales. Points indicate nodes, while red lines connect nearest nodes (Pasyanos et al., 2014) .....	18
Figure 3.1: Point sample from surfer software .....	20
Figure 3.2: Shows the constituents of the litho 1.0 file .....	22
Figure 3.3: Shows the edited makefile .....	23
Figure 3.4: Shows sample of the Litho 1.0 crustal density .....	24
Figure 3.5: Shows the window for the inputs during conversion of grid to binary formats .....	25
Figure 3.6: Shows the interface of TGF with inputs for computations of terrain correction .....	27
Figure 4.1: Shows the variation of free-air gravity anomalies .....	34
Figure 4.2: Shows the variation of bouguer gravity anomalies over AOI .....	36
Figure 4.3: Shows the variation of second computed bouguer gravity anomalies .....	38
Figure 4.4: Relief map shows variation of the third computed bouguer gravity anomalies .....	40
Figure 4.5: Relief map showing the variation of computed bouguer gravity anomalies .....	42

## List of Tables

Table 3.1:Distribution of DEMs as used in TGF software in computations of terrain corrections .....	28
Table 3.2: A sample of computation points used in computation of terrain corrections .....	28
Table 3.3: Show the statistics used for validations of results .....	29
Table 4.1: Shows values of normal gravity at reference ellipsoid.....	32
Table 4.2: Shows sample of the computed free-air gravity anomaly .....	33
Table 4.3:Bouguer gravity anomalies when R1 was kept at approximately 3.5km and R2 at approximately 90km .....	35
Table 4.4:Computed gravity anomalies whenR2 is kept approximately at 80km while R1 was kept at 3.5km.....	37
Table 4.5: R2 is kept approximately at 90km while R1 was kept constant at 5km .....	39
Table 4.6: R2 is kept approximately at 80km while R1 was kept constant at 5km .....	41
Table 4.7: Shows the validation results of bouguer anomalies.....	43
Table 4.8: Shows the validation of free-air anomalies .....	43

## **List of the Abbreviations**

AOI	Area of Interest
ALOS	Advanced Land Observing Satellite
ARU	Ardhi University
DEM	Digital Elevation Model
DGST	Department of Geospatial Sciences and Technology
GUI	Graphical User Interface
MATLAB	Matrix Laboratory
SRTM	Shuttle Radar Topographic Mission
mGal	Miligals
TZG07	Tanzania Geoid Model 2007
TZG08	Tanzania Geoid Model 2008
EGM08	Earth Gravity Model 2008
SA	Satellite Altimetry
IUGG	International Union of Geodesy and Geophysics
STD	Standard Deviation
RMS	Root mean square

# **CHAPTER ONE**

## **INTRODUCTION**

### **1.1 Background**

Zanzibar is a composition of many isles with two huge and common habitable isles namely Unguja and Pemba. In the earth's gravity field, geoid provide good representation of features with high wavelengths but the problem is encountered for those with short wavelengths, this have resulted using of the surface gravity which is the best way of presentation of the features with short wavelengths compared to the using of the geoid (Hoffman-Wellenhof & Moritz, 2005). This has led to the reason why Geophysicists are more interested in gravity because it allows them to learn about inner earth density distribution. To learn about earth's interior, we must deal with the problem of observing gravity in inner parts of the earth. A worldwide gravity data is maintained by Bureau Gravimetrique International in Paris, an institution of IUGG (Vanicek, 1986).

Gravity anomalies are variations in the Earth's gravitational field caused by variations in the density distribution of subsurface materials. One significant type of gravity anomaly is the Bouguer gravity anomaly, named after Pierre Bouguer, a French mathematician and physicist who made important contributions to the field of geodesy and gravity studies. Gravity anomaly may be referred as the difference between reduced actual gravity and normal gravity on ellipsoid. This deviation of the gravity caused the variation of the density or composition of the earth's crust and upper mantle. There are several types of the gravity anomalies such as free-air gravity anomaly, bouguer gravity anomaly etc. (Petr & Edward, 1986)

Bouguer gravity anomaly takes in to account effects of the topography above the reference ellipsoid while free-air gravity anomaly takes into account effect of the earth's atmosphere above reference ellipsoid. These types of the anomaly play great roles in geophysical activities, geodesic activities etc.

In order to obtain gravity in the interior of the earth we have to apply some reduction to the observed surface gravity and reduce it to the reference ellipsoid. These reductions are free-air surface reduction and bouguer reduction. If we assume that there is only air between reference ellipsoid and the surface where the gravity has been observed i.e., those masses between ellipsoid and surface have been mathematically removed, the effect to the surface gravity observed caused

by the air between ellipsoid and observed point is what is called free-air correction. To remove this effect, we are supposed to create what is called free air anomaly.

Also, topography provide huge effect to the gravity so in order to obtain the gravity at geoid we must take into account the issue of effect of topography situated between ellipsoid and surface. This is referred as bouguer reduction in which effect of the attraction of the earth topography between ellipsoid and observed gravity is subtracted. To subtract the effect of topography from free-air anomaly is what is referred as bouguer anomaly (Hoffman-Wellenhof & Moritz, 2005).

Gravity measurement can be of many uses such as natural hazard assessment and understanding earth's rotation but mainly can be used for geoid determination. In order to be able to uses the gravity measurement for geoid determination, database of gravity containing all gravity spectrum is needed (Peter, 2018).

Different researches have been conducted in Tanzania to create different gravity databases. For example, Busega & Kimboi (2018) created a 1'x1' quality surface gravity anomaly database optimally incorporating all the relevant current sources for the area of interest (AOI) of Tanzania which was then validated by using 56 reference gravity stations yielded RMS value of 17.27 mGal, mean value of -5.3306mGal, minimum and maximum values of -42.09mGal and 25.64mGal respectively.

Furthermore, Nchambi (2021) developed gravity database TGDB21, comprised of gravity data covering the East African region. TGDB21 has 95489 Point gravity data, 42562 AGP 5'X5' gravity anomaly and the 1'X1' free-air marine gravity anomaly cleaned at 99% confidence interval. The database met the requirements of being used for many various applications. TGDB21 had five tables for storing data, five queries for computing the gravity anomalies and reductions and five forms for entering and displaying the gravity data.

In the context of gravity anomalies in Zanzibar, the only existing database is the one specifically developed for surface gravity anomalies. Mussa (2022) created surface gravity anomaly database for Zanzibar, the validation of both surface gravity anomalies and the actual surface gravity anomaly at the point gravity stations over the AOI were performed at 95% confidence level. Validation of the result yielded Mean, Standard Deviation and Root Mean Square statistics of the differences as 8.823 mGal, 7.506 mGal and 11.395 mGal respectively.

As it can be seen from previous created databases, mostly were aimed on surface gravity anomalies and free-air marine gravity anomaly but due to development of sciences and technology demand to accurately developing the bouguer and free-air gravity anomaly database is huge. Therefore, the study aimed to create both classical bouguer and free-air gravity anomaly databases in Zanzibar.

Listed below are some of the applications of the gravity reduction. (Hoffman-Wellenhof & Moritz, 2005).

- i. Determination of the geoid
- ii. Gravity prediction and densifications
- iii. Monitoring of the earth's crust

## **1.2 Problem statement**

The lack of classical bouguer and free-air gravity anomaly databases is hindering progress in the field of geophysics and geodesy in Zanzibar. Despite the important role that these databases play in understanding the earth crust movements, investigating hazards etc. there is still no availability of these databases for researches. This is resulted into limited availability of data, lack of consistence of the data available making it difficult to compare results from different studies regarding to these anomalies. The findings will play great roles in hazard assessments, mineral explorations and many other positive impacts to the society.

## **1.3 Objectives**

### **1.3.1 Main objectives**

The main objective of this research is find optimal method for creation of classical bouguer and free air gravity anomalies database.

### **1.3.2 Specific objective**

- a) To compute most accurate value for bouguer corrections.
- b) To compute most accurate values for terrain corrections.
- c) To compute most accurate values for free-air gravity corrections.

## **1.4 Significances**

- a) Plays a great role in identifying potential hazards, example landslides and fault lines around the areas.



- b) Infrastructures planning such as pipeline networks, networks should avoid potential problem caused by subsurface structures.
- c) Exploration of minerals.

## **1.5 Output**

This study aimed at determining optimal method for creation of classical bouguer and free-air gravity anomalies databases which can bring the many positive impacts to the society such as helping in resources exploration in the ground and hazards assessments.

## **1.6 Scope and limitations**

Due limited time of the study, we are going to focus only in Zanzibar islands and data to be used is surface gravity data from the recently computed 2022 1'×1' surface gravity anomaly since it is most current database obtained.

## **1.7 Beneficiaries**

- a. In Geodynamics

Gravity information obtained can be used to explain about deformation of AOI

- b. In Geomatics

Gravity anomalies can be used in transformation of data to mappings, height systems and so on.

- c. In Geodesy

In this field it can be helpful in geoid computation, vertical datum unifications etc.

- d. In Geophysics

It can be used in determination of the hazards such as landslides.

## **1.8 Study area**

Zanzibar is located in east Africa along the coast of Indian Ocean. It situated about 25-50 kilometers off the coast of Tanzania located between latitude 6° to 8° south and 39° to 41° east. Unguja has about 93 kilometers (58 miles) long and 30 kilometers (19 miles) wide which sum up of total area of approximately 1,461 square kilometers (637 square miles), it is most populated island in Zanzibar while Pemba has about 63 kilometers (39 miles) long and 23 kilometers (14 miles) which sum up an approximately area of 988 square kilometers (381 square miles).

## **1.9 Dissertation Outline**

This dissertation is organized in five chapters as follows.

Chapter one begins with a background of the dissertation. It also consists of the statement of the problem, objectives, output, significance and beneficiaries.

Chapter two describes about the situation of gravity in Zanzibar followed by explanation about gravity anomaly and ending with deep explain about gravity reductions i.e. free-air reductions and bouguer gravity reductions.

Chapter three details on methodology of the dissertation by describing all relevant datasets, procedures and mathematical models required to achieve the objective of the study, i.e., optimal method for creation of classical bouguer and free-air gravity anomaly database.

Chapter four gives all the numerical and mapping results from the processing of data outlined in the methodology part, it is also in this chapter where the results are analyzed and discussed.

Chapter five consists of conclusion and recommendations. Conclusion summarizes dissertation findings in view of the dissertation problem followed by recommendations to be considered by future dissertators.

## **CHAPTER TWO**

### **LITERATURE REVIEW**

#### **2.1 Situation of gravity in Zanzibar.**

Zanzibar is a composition of isles found in Tanzania, the country among the few African countries with almost all types of gravity data such as satellite, terrestrial, marine altimetry and aerial gravity. There are different organization with in Tanzania and oversee which maintain the gravity data. The following are some of the Tanzanian organization which maintain and stores the gravity data.

- i. Ministry of minerals and energy
- ii. Ministry of Land, Housing and Human settlements developments
- iii. Ardhi University under Department of Geospatial Sciences and Technology (DGST)
- iv. University of Dar Es Salaam under Department of Geology.

Some of the oversees organizations which stores the gravity data

- i. Gravity and Geoid for Africa (GGA)
- ii. USA National Geospatial Agency (NGA)
- iii. Global Exploration Technology (GETECH), it provides the gravity data for Oil and mineral exploration and also for dissertation purposes.
- iv. Danish National Space Centre (DNSC) of the Technical University of Denmark (DTU) which provides the satellite altimetry marine gravity data.

Zanzibar is part of Tanzania which is among the few African countries that have almost all sources of gravity data such as terrestrial, satellite, altimetry and marine gravity data. The current situation of gravity data found in Zanzibar is briefly explained in this section.

#### **A. Terrestrial point gravity**

This refers to gravity stations without monument on the earth's surface. Most of ground gravity which covers Zanzibar has been observed for oil and gas exploration. Observations shows that there is no any terrestrial point gravity in Pemba island while there are some points distributed in Unguja island. These gravity station found in Unguja were mainly obtained through the oil exploration process. The Figure 2.1 below shows the distribution of the gravity stations in Zanzibar.

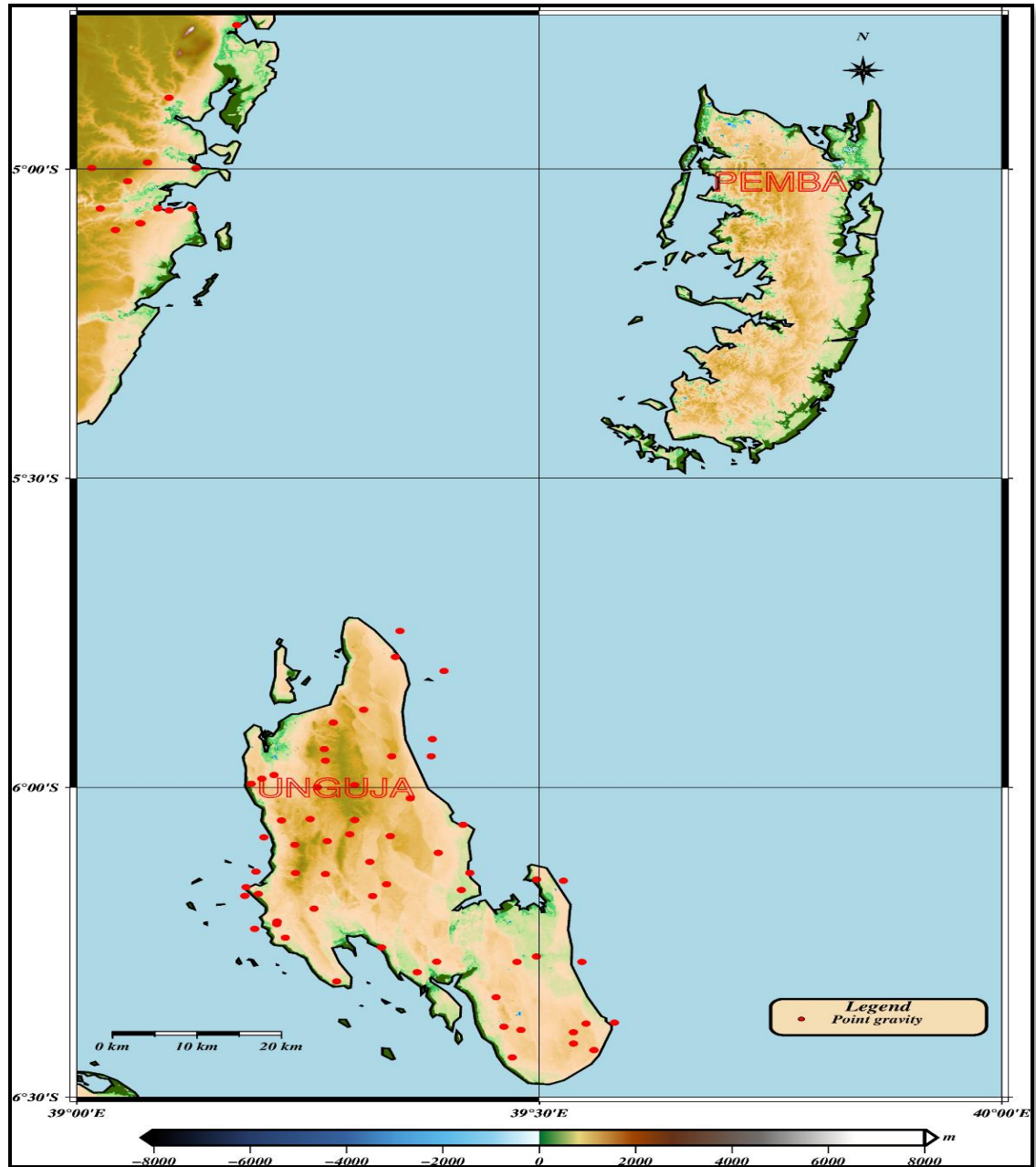


Figure 2.1: Distribution of gravity station in Zanzibar (Mussa, 2022)

## B. Terrestrial ground gravity

This refers to gravity stations with monuments on the earth's surface, these stations have been established since 1954 by various exploration companies for oil and gas exploration. There are only two terrestrial ground gravity points in Zanzibar which found in the airfields. The first one is

found at Abeid Amani Karume airport in Unguja and the second one is found in Pemba airport. The Figure 2.2 belows shows the location of the terrestrial ground gravity in Zanzibar.

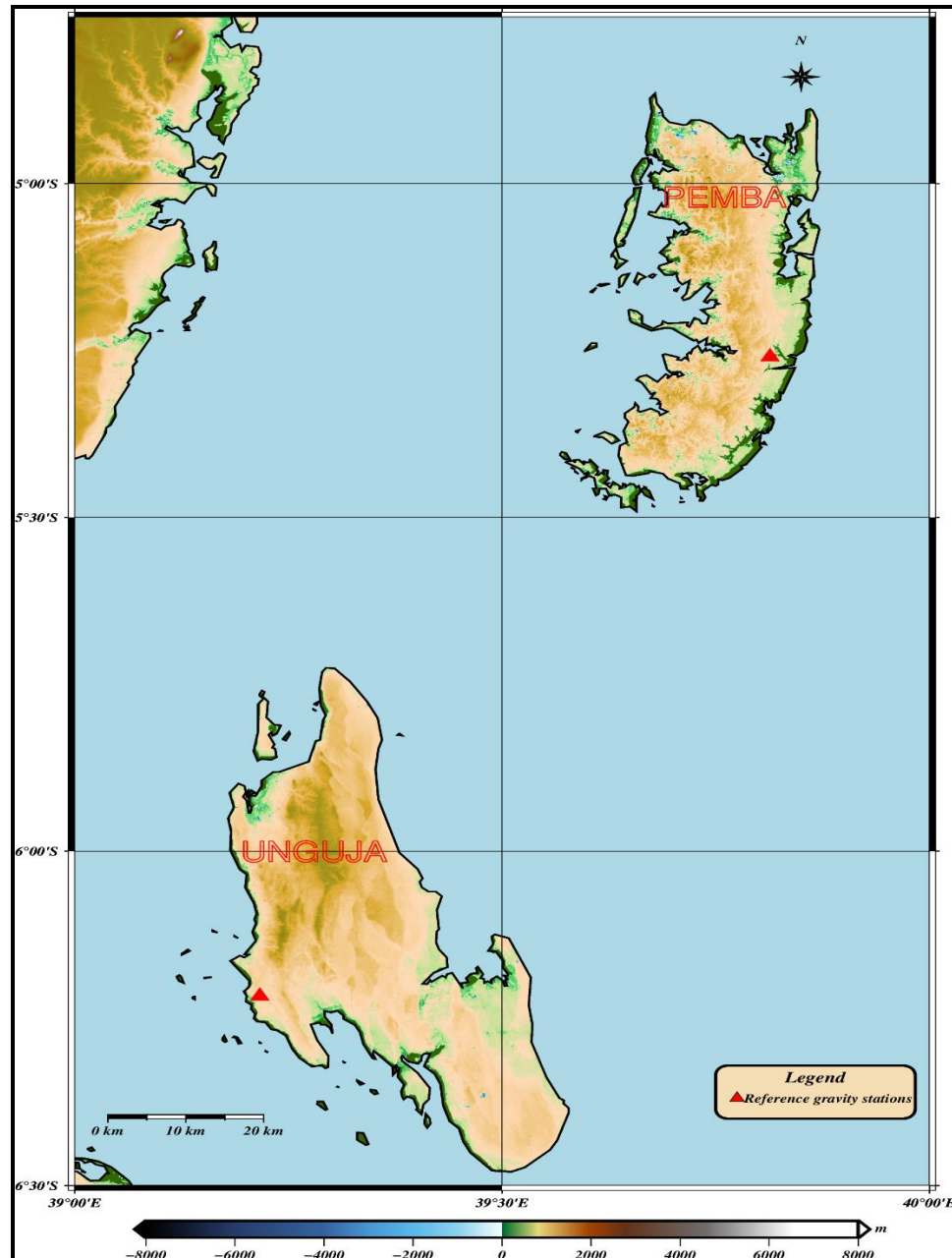
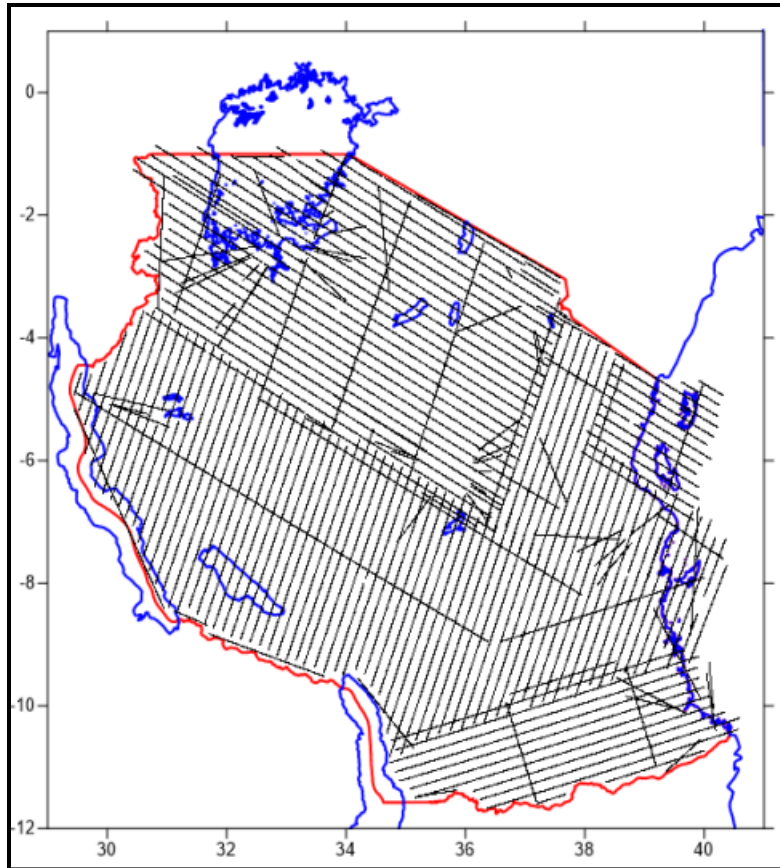


Figure 2.2 Shows the location of the terrestrial ground gravity in Zanzibar (Mussa, 2022)

### C. Aerial gravity

The aerial gravity observation in Tanzania was completed in 2013 under the project between the Technical University of Denmark (Danmarks Tekniske Universitet (DTU)) (as a contractor) and the Ministry of Lands, Housing and Human Settlements Development of Tanzania; Surveys and

Mapping Division (MLHSD-SMD) (as a client). A 5'×5' surface aerial gravity anomaly of about 5mGal precision covering the whole of Tanzania geographical boundary was produced as seen in Figure 2.3 below show the distribution of the aerial gravity.



*Figure 2.3 Aerial gravity data in Tanzania*

## 2.2 Gravity anomaly

Gravity anomaly  $\Delta g$  refers to the difference between the reduced actual gravity  $g$  and the normal gravity at reference ellipsoid  $\gamma$ . Through the different observations shows that the value of the gravity varies depending on the several factors such as different heights of the observation points, oblateness and uneven distribution of the mass on the earth. The treatment of the observed gravity based on those factor rises to different kind of the gravity anomalies such as free-air gravity anomaly, bouguer gravity anomaly and surface gravity anomaly. The globally range of the variation of the gravity is more than 5Gal which is approximately about 0.5% of average  $g$ , this variation can be detected even by imprecise instruments. (Vanicek, 1986)

The diagram below shows the illustration of the gravity anomaly.

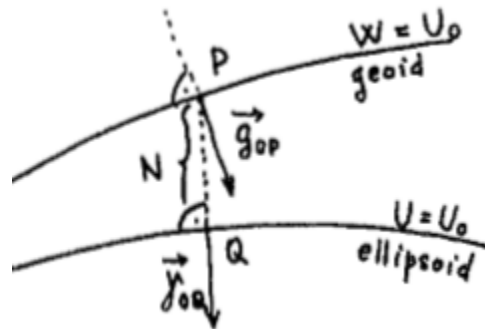


Figure 2.4 Shows the illustration of the gravity anomaly (Vanicek, 1986)

$$\Delta g = g_p - \gamma_Q \dots\dots\dots (2.1)$$

Where by

$\Delta g$  stands for gravity anomaly between two reference surfaces

$g_p$  stands for actual gravity at point p on the geoid

$\gamma_Q$  stand for normal gravity at point Q on the ellipsoid

### Application of the gravity anomaly

- d) potential hazards identifications and determinations, example landslides and fault lines around the areas.
- e) Infrastructures planning such as pipeline networks, networks should avoid potential problem caused by subsurface structures.
- f) Exploration of minerals.
- g) Hazards assessments such as faults and landslides.

## 2.3 Gravity reductions

Observation of the gravity  $g$  is not done on the geoid but on the masses above geoid so whenever we want to obtain the value of the gravity  $g$  on the geoid we are supposed to implement some reduction on the value of the observed gravity. These reductions are dependent upon the way of dealing with topographic masses above geoid. There are two ways of dealing with topographic masses above geoid (Hoffman-Wellenhof & Moritz, 2005).

- i. Completely removal of the topographic masses above the geoid or shifted below the geoid.
- ii. Gravity station is lowered from the point on the surface of the earth to the point on the geoid

If we consider completely removal of the topographic masses above the geoid, we are supposed to deal with density models since the density varies as we move down the crust and for the issue of lowering the gravity station to the geoid we are supposed to deal with vertical gradients from the point on surface of the earth to the point on the geoid.

The way of dealing with topographic masses give rise to the different types of the reductions such as free-air reductions, bouguer reductions and Poincare reductions.

Functions of the gravity reductions

- a. Geoid determinations.
- b. Interpolation and extrapolation of the gravity.
- c. Investigation of the earth's crust.

### 2.3.1 Free-air reduction

In this type of the reduction we assume that there are no topographic masses above the geoid, this reduction only account only for the effect of the height above the geoid to the point where the gravity has been observed. In order to reduce effect of the free-air above the geoid we are supposed to apply the free-air correction  $dg/dH$  to the value of the observed gravity  $g$  (Hoffman-Wellenhof & Moritz, 2005).

$$\frac{dg}{dh} = \frac{-2GM}{r^3} \dots\dots\dots (2.2)$$

G stands for the gravitational force of the attraction



M stands for mass of the earth

r stands for radial distance from the center of mass

limiting the value of the r to the surface of the earth i.e. r is equal to radius mean earth sphere, the value of  $dg/dh$  will be

$$\frac{dg}{dh} = -0.3086$$
$$dg = -0.3086dh \dots\dots\dots (2.3)$$

Note that,  $dg$  will always be positive for negative values of  $dh$  i.e. increasing of  $dh$  decreasing of  $dg$  and vice versa. Therefore, it can be written as:

$$g_0 = g_p - 0.3086dh \dots\dots\dots (2.4)$$

Where by,

$g_0$  stands for reduced gravity at geoid

$g_p$  stands for gravity value at surface of the earth

$dh$  stands for increments in vertical

### 2.3.2 Bouguer reduction

The main objective of bouguer reduction is completely removal of topographic masses above the geoid. For this case, there will be either incomplete bouguer reduction, complete bouguer reductions and simple or refine bouguer reductions (Hoffman-Wellenhof & Moritz, 2005).

#### **Bouguer plate:**

Let's assume that the mass above the geoid i.e. bouguer plate is plane or completely horizontal with constant density  $\rho$ , then it follows that the attraction forces A of bouguer plate obtained from calculus is given as

$$A_B = 2\pi G\rho H \dots\dots\dots (2.5)$$

Where by

$A_B$  stands for bouguer attraction

$G$  stands for gravitational force of attraction

$\rho$  stands for density of topography above geoid

$H$  stands for the thickness of the bouguer plate

Given the constant value of the density  $\rho$  equal to  $2.67g/cm^3$  will result to

$$A_B = 0.1119H \dots\dots\dots (2.6)$$

Note: the formula is obtained by considering shape of the bouguer plate to be circular cylinder. If the bouguer plate is considered to be spherical then we will have to replace  $2\pi$  by  $4\pi$ .

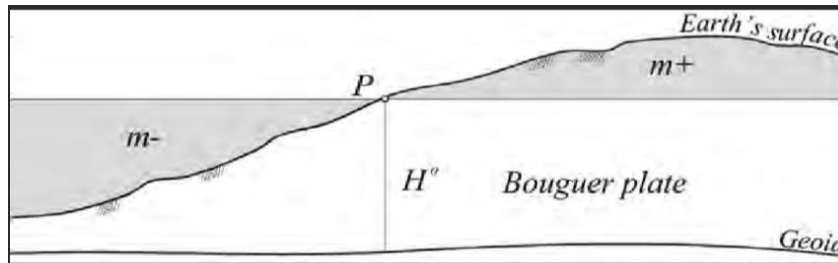


Figure 2.5 Bouguer plate

Removing the effect of bouguer attraction to the value of observed gravity  $g_p$  is known as incomplete bouguer

i.e.  $g_B = g_p - A_B \dots\dots\dots (2.7)$

where by

$g_B$  stands for bouguer gravity

$g_p$  stands for observed gravity at point p on surface

$A_B$  stands for bouguer plate attraction.

Furthermore, to complete bouguer reduction we are supposed to consider the effect of free-air observed gravity. Since the effect of free-air increase as H decreases then we will add free-air correction to the value of the bouguer gravity. The equation will be:

$$g_B = g_p - A_B + F \dots\dots\dots (2.8)$$

Numerically,

$$g_B = g_p + 0.196H \dots\dots\dots (2.9)$$

This is referred as complete bouguer reduction

### 2.3.3 Terrain correction

This is type of correction which is supposed to take into account because simple bouguer does not remove precisely effect of the topography. This correction takes in to account the deviation topographic masses from bouguer plate. Hence it is called terrain topographic correction  $A_t$  (Vermeer, 2020).

Since the topographic masses above the bouguer plate are removed then the terrain correction is always positive. Mathematically, the equation will become:

Consider the diagram below

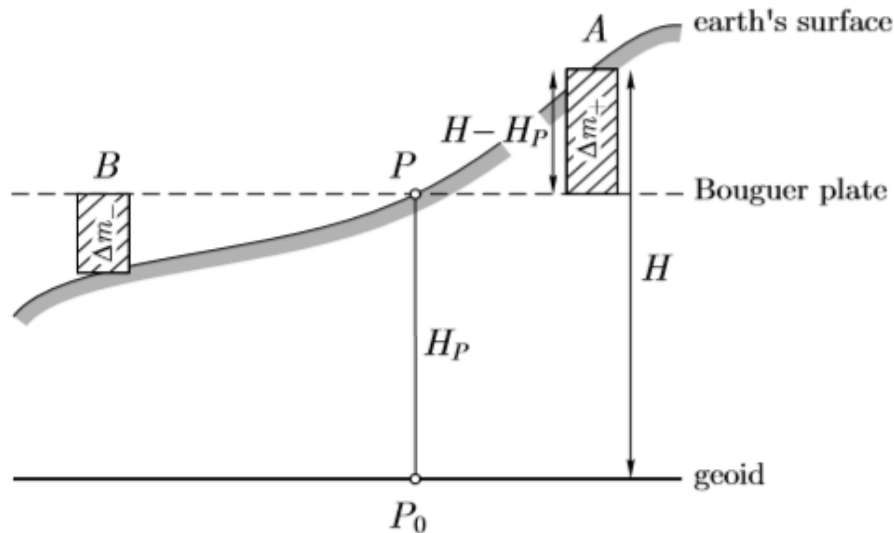


Figure 2.6 Terrain correction (Hoffman-Wellenhof & Moritz, 2005).

At point A, the mass surplus  $\Delta m_+$  which attracts upward is removed, causing  $g$  at P to increase. At B the mass deficiency  $\Delta m_-$  is made up and causing  $g$  at P to increase. Therefore, the terrain

effect is always positive (Hoffman-Wellenhof & Moritz, 2005). The equation below shows refined bouguer reduction.

$$g_B = g_p - A_B + F + A_t \dots\dots\dots (2.10)$$

Whereby;

$g_B$  stands for bouguer gravity

$g_p$  stands for observed gravity at point p on surface

$A_B$  stands for bouguer plate attraction

$F$  stands for free-air corrections

$A_t$  stands for terrain corrections.

Terrain corrections are computed using TGF software which is based on the complex integration. The integral is numerically evaluated by using a Digital Terrain Model (DTM). This can be done using FFT methods in planar approximation.

### 2.3.4 Poincare and Prey reduction

The reduction deals with the fact that the gravity value inside the earth cannot be measured physically, so we are obtaining the value of the gravity inside the earth by reducing the value of the gravity observed by using Poincare and prey reduction. (Hoffman-Wellenhof & Moritz, 2005)

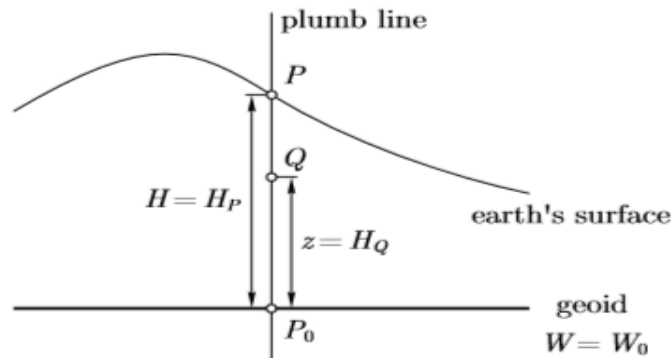


Figure 2. 7 Prey reduction (Hoffman-Wellenhof & Moritz, 2005).

According to the Poincare and Prey method, the formula below is used.

$$g_Q = g_p - \int_Q^P \frac{\partial g}{\partial H} dH \dots\dots\dots (2.11)$$

## 2.4 Overview of density models

Most of the gravimetric terrain reduction methods require the density of the crust to be known in order to compute the topographic effects on the gravity field quantities. In the absence of a distributed crust density model, a mean density value of  $\rho_c$  is often used in geodetic and geological activities (Tenzer et al., 2011). Although this value is widely used, its origin remains partially obscure (ibid). This value was only the approximate of density in terrain composed of crystalline. (Hinze, 2003). However, roughly only of the continental surface is crystalline, while other (is underlain by sedimentary rocks (ibid).

Over the last three decades, several global crustal density models were obtained by means of seismic velocities. These models include the CRUST series from CRUST5.1, CRUST2.0 to CRUST1.0 published by the US Geological Survey and the Institute for Geophysics and Planetary Physics at the University of California. The suffix represents the resolution of the given models in degrees. Using CRUST1.0 (Laske et al., 2013) constructed a  $1^\circ$  tessellated global model of the crust and lithospheric model of the Earth (LITHO1.0).

### 2.4.1 CRUST1.0 density model

CRUST1.0 is a global crustal model at  $1^\circ \times 1^\circ$  resolution which was formally released by (Laske et al., 2013). As an update version of CRUST5.1 and CRUST2.0, it incorporated a wealth of newly available data on global surface topography, seafloor bathymetry, seismic refraction, as well as the thickness data of ice, sediment and the crust. This model consists of 64800  $1^\circ \times 1^\circ$  cells arranged in a fixed latitude-longitude grid (ibid). In each cell, the Crust is described vertically by eight geophysical identified sub layers: (1) water, (2) ice, (3) upper sediments, (4) middle sediments, (5) lower sediments, (6) upper crust, (7) middle crust, and (8) lower crust. The model included water and ice as the first two sub layers so as to make it as complete as possible (Mooney et al., 1998; Laske et al., 2013). For each sub layer, the boundary depth and physical properties, including density  $\rho$ , compressional wave velocity  $V_p$ , and shear wave velocity  $V_s$  are specified to depict the variation of the crustal thickness and associated properties.

This model uses Bathymetry and topography data provided by ETOPO1 (Amante & Eakins, 2009) whose horizontal datum is WGS84 geographic and vertical datum is the sea level. The topography, bathymetry and ice thickness in this model were thus derived from ETOPO1 by binning and averaging the data in 1- degree cells.

In order to access density at a certain longitude and latitude in the CRUST1.0 model, the FORTRAN source code were given which can be compiled with any Fortran 77 compiler (Laske et al., 2013).

#### **2.4.2 Litho 1.0 crustal density model**

The LITHO1.0 model is a  $1^\circ \times 1^\circ$  tessellated model of the crust and uppermost mantle of the Earth, extending into the upper mantle to include the lithospheric lid and underlying asthenosphere (Pasyanos et al., 2014). This model was developed from CRUST1.0 model and incorporated more types of newly available data. This model is parameterized (horizontally and vertically) in such a way to make it suitable for geophysical computations on the sphere. Lateral parameterization is defined with a spherical tessellation surface, while depth parameterization is achieved through thickness and associated parameters (density,  $V_p$ ,  $V_s$ ,  $Q$ ) of the layers (ibid).

The model is parameterized laterally as tessellated surface rather than on fixed grid of latitude and longitude so as to make more evenly samples on the globe. This tessellation was achieved by first constructing a regular polyhedron with 20 equilateral triangular faces, 30 edges, and 12 vertices, which are approximately  $60^\circ$  apart (ibid). Each triangle was then subdivided into four daughter triangles, halving the node separation each time until the desired spacing was achieved. With six subdivisions ( $60^\circ \rightarrow 30^\circ$ ,  $30^\circ \rightarrow 15^\circ$ ,  $15^\circ \rightarrow 8^\circ$ ,  $8^\circ \rightarrow 4^\circ$ ,  $4^\circ \rightarrow 2^\circ$ ,  $2^\circ \rightarrow 1^\circ$ ) of the starting object, 40,962 vertices and 81,920 triangles at approximately  $1^\circ$  were created. In comparison, a  $1^\circ$  regular grid in latitude and longitude would have significantly more points (64,800) but more closely sampled at the poles. Example of the tessellated nodes on global and regional scales is shown in Figure 2.8.

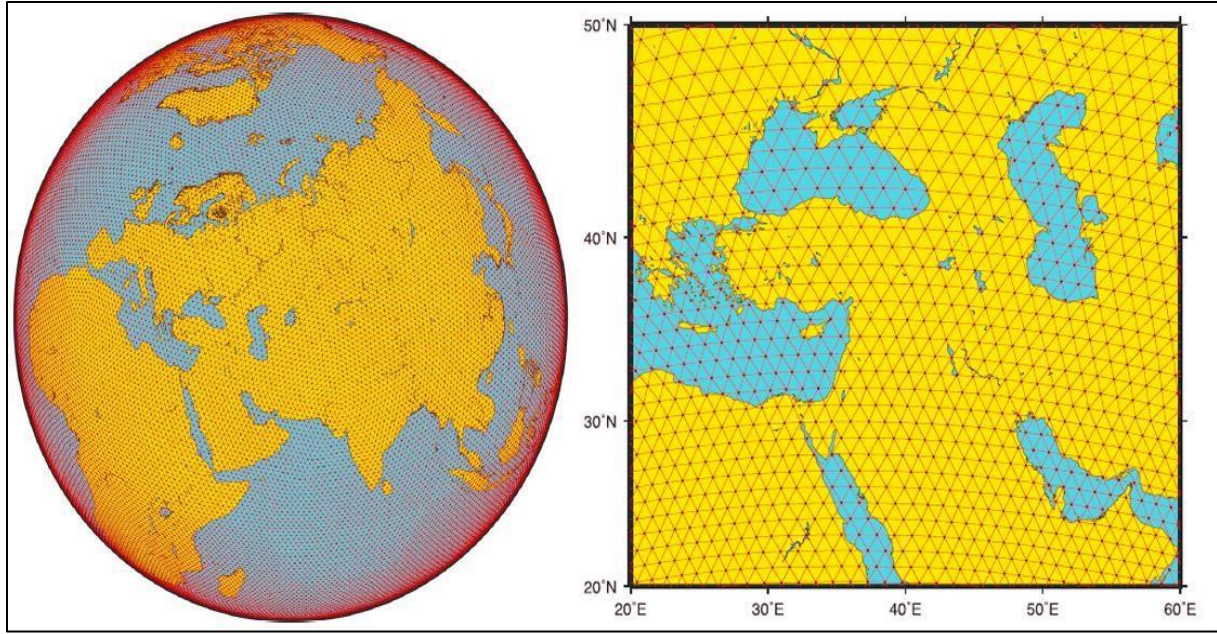


Figure 2.8 Lateral parameterization at tessellation on the global (left) and regional (right) scales.

Points indicate nodes, while red lines connect nearest nodes (Pasyanos et al., 2014). The model is parameterized vertically as a series of geographically identified nine sub layers, which are (1) water; (2) ice; (3) upper sediments; (4) middle sediments; (5) lower sediments; (6) upper crust; (7) middle crust; (8) lower crust; and (9) lithospheric mantle (lid). Each layer has a thickness and associated parameters such as velocity ( $V_p, V_s$ ), density and Seismic attenuation. Figure (2.8) shows the arrangement of the sub layers.

This model adopted the bathymetry and topography data of CRUST1.0 which were provided by ETOPO1 (Amante & Eakins, 2009). Its horizontal datum is WGS84 geographic and vertical datum is the sea level. The topography, bathymetry and ice thickness in this model were derived from ETOPO1 by binning and averaging the data in 1- degree cells (Pasyanos et al., 2014).

## CHAPTER THREE

### METHODOLOGY

In this chapter, the data types used were explained in details, the preprocessing of these data, and the methodologies employed in the analysis of both the free-air and Bouguer gravity anomaly databases. Specifically, when computing the Bouguer corrections, particularly terrain correction, several authors have developed methods that utilize computer availability and Digital Terrain Models. These methods involve implementing a model of rectangular prisms of mass elements to compute the integration of terrain correction.

#### 3.1 Computation of free-air gravity anomaly grid from ground gravity points.

Ground gravity data of the area of the interest AOI were obtained from Ardhi University database (DGTB21) which was determined by (Mussa, 2022). By using those points and Digital Elevation Models, the following procedures were followed during computation of the free-air.

By definition;

$$\Delta g_{FA} = g_{FA} - \gamma_0 \dots\dots\dots (3.1)$$

Whereby;

$g_{FA}$  stands for reduced free-air gravity

$\gamma_0$  stands for normal gravity at reference ellipsoid.

In order to obtain the reduced free-air gravity from the given point gravity data, points gravity of AOI were reduced from the effect of free-air by considering the elevation. These have been done using the formula below

$$g_{FA} = g_p - 0.3086dH \dots\dots\dots (3.2)$$

To obtain the value of the  $g_{FA}$ , Digital Elevation Model was used for provision of elevation so as come up with the reduced free-air gravity.



The Digital Elevation Model (DEM) of ALOS v3.1-1 was initially imported into Global Mapper software to convert it to the Gravsoft grid format for area of interest. This DEM is primarily used to obtain the elevation values (orthometric height) for corresponding gravity points. Subsequently, the grid format of the ALOS v3.1-1 DEM was opened in Surfer software, and the elevation of point gravity was extracted using the point sample window as shown in Figure 3.1 below.

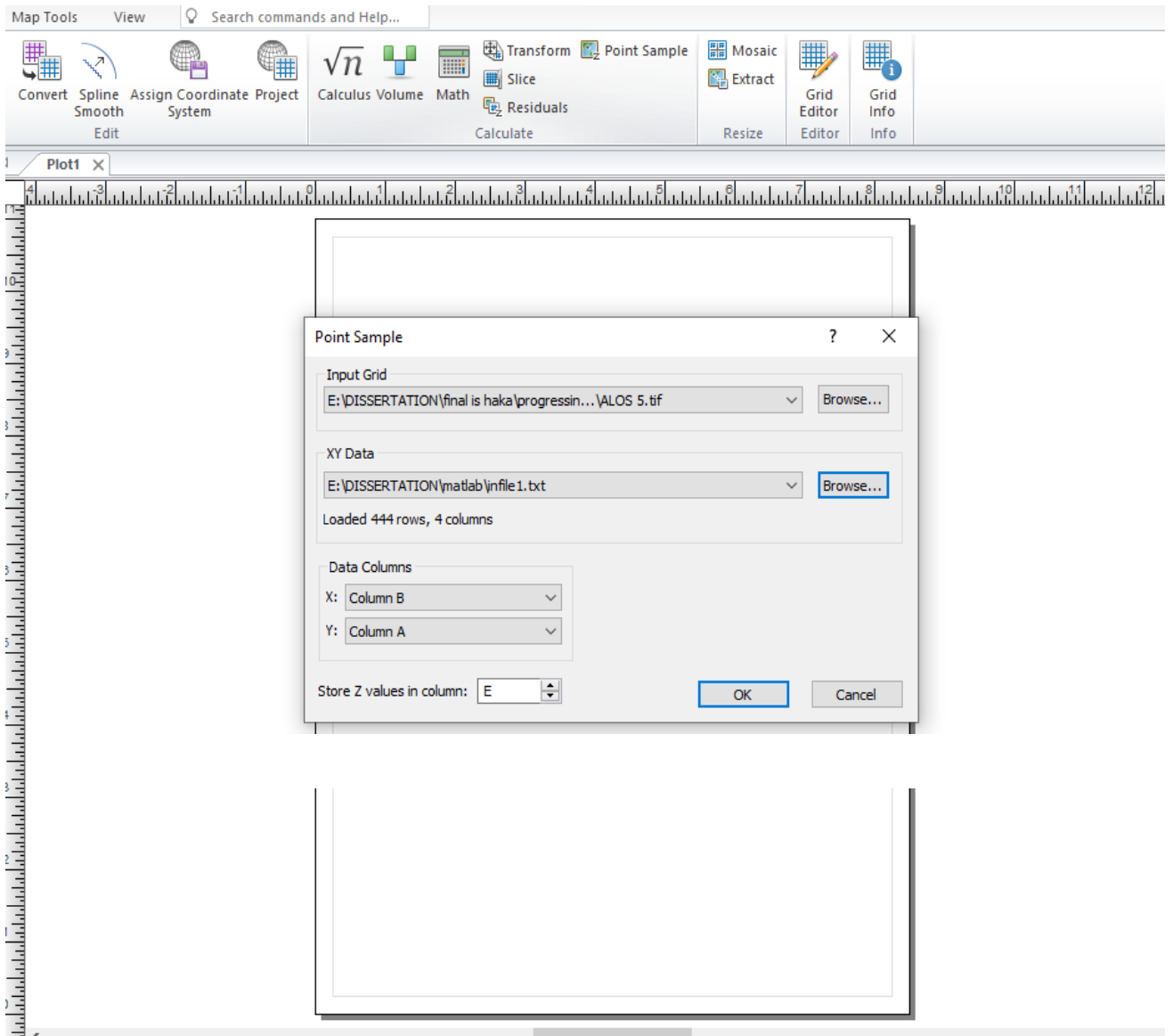


*Figure 3.1: point sample from surfer software*

The output file consists of longitudes, latitudes and orthometric heights of the gravity points.

The computation of the free-air gravity anomalies was done using MATLAB software by using the codes that was developed by Busega & Kimboi (2018) which required the input file of phi, lambda, H and g in text format. The file was saved as input.txt and recalled in MATLAB for computation. After running the codes, the computation started by computing the normal gravity at the reference ellipsoid, followed by the free-air gravity anomaly.

### 3.2 Computation of the bouguer gravity anomalies.

In this research, refined bouguer gravity anomalies were computed which consist of the bouguer attraction correction, free-air as well as terrain corrections. Terrain corrections intends to deal with effects of the topographic masses deviated from bouguer plate. Terrain correction have been computed using different approaches by using variable density model of LITHO1.0 to observe which among those approaches would results into best bouguer gravity anomalies. Also variation of integration radius of detail and resolution of DEM used.

$$\Delta g_B = g_p - A_B + g_{FA} + T_C - \gamma \dots\dots\dots (3.3)$$

Whereby:

- $g_p$  stands for point gravity
- $g_B$  stands for bouguer gravity
- $A_B$  stands for bouguer plate attractions
- $g_{FA}$  stands for free-air reduction
- $T_C$  stands for terrain correction
- $\gamma$  stands for normal gravity at reference ellipsoid.

#### 3.2.1 Obtaining crustal density data from LITHO1.0 density model.

The LITHO1.0 is contained in uncompressed file with extension .tar file, which contains the README file and the LITHO1.0 file. Within the LITHO1.0 file, there are two subdirectories: "progs" and "litho\_models." The "progs" directory contains files with C++ codes that have been executed to access the LITHO1.0 data.

By using README file, first we were supposed to create bin file where the accessed data will be stored, then to adjust makefile directory for the BIN, FLAGS and CPP. After those adjustments we run the access\_litho. All these steps were implemented using command prompt with support of C++ compiler installed. Figure 3.2 below is how LITHO1.0 file were seen.

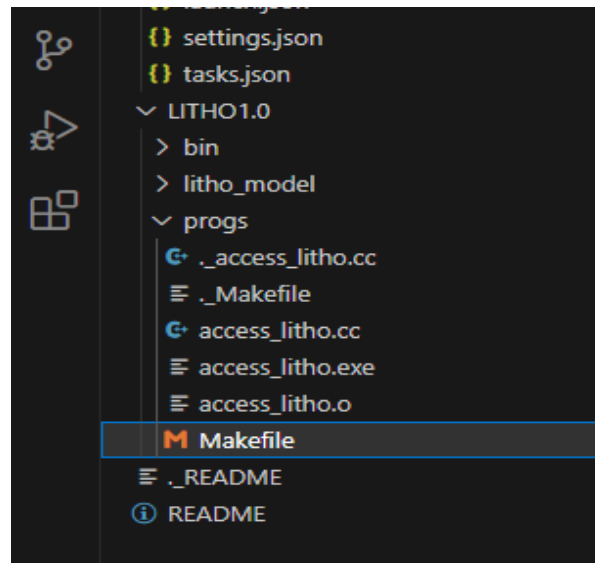


*Figure 3.2: Shows the constituents of the litho 1.0 file*

After creating the bin file as seen in the Figure 3.2 above, then the makefile was adjusted as shown in the Figure 3.3 below. Those directories were adjusted according to the examples shown in the README file.

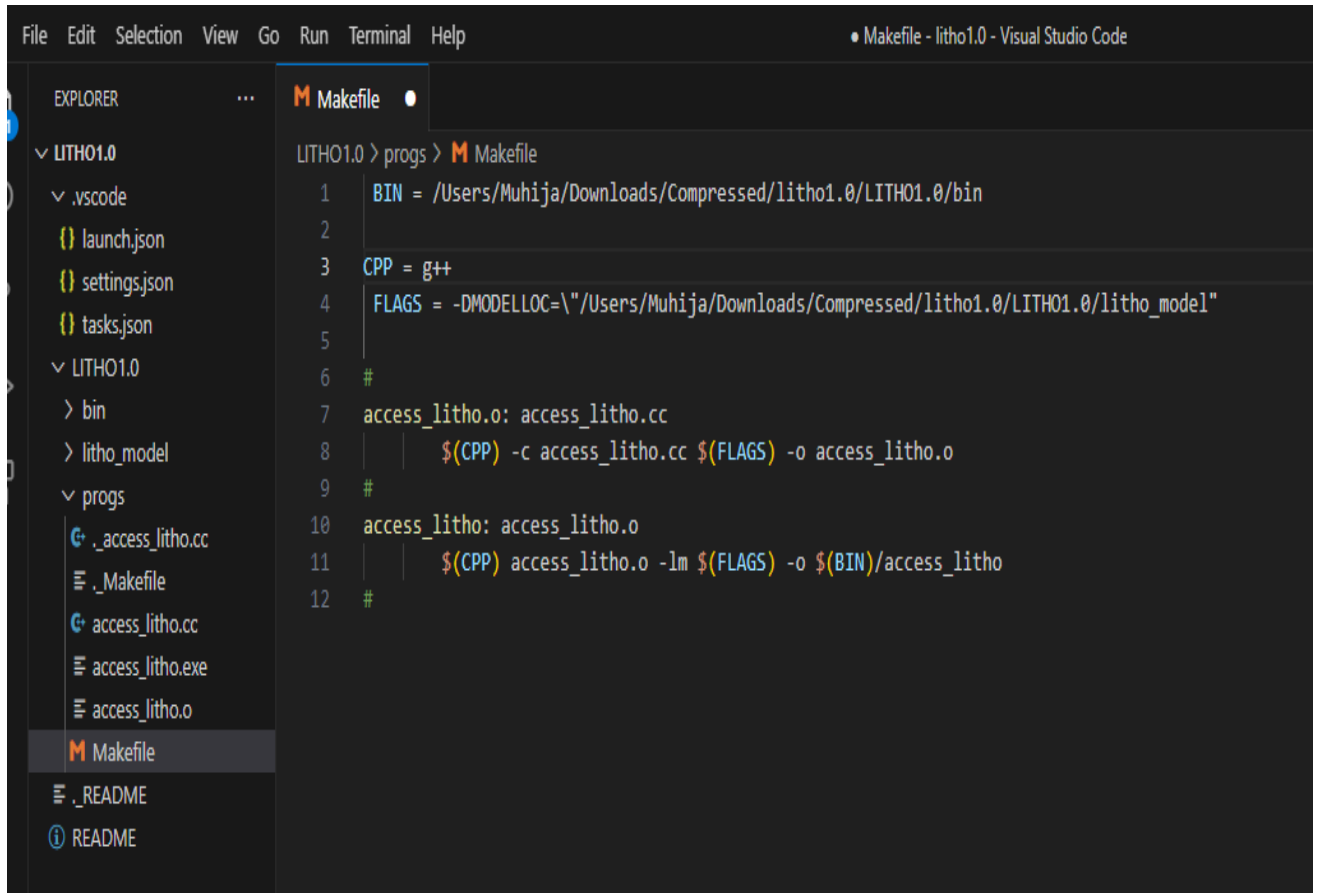


*Figure 3.3: Shows the edited makefile*

Lastly,  $1^{\circ} \times 1^{\circ}$  grid cells (nodes) of LITHO 1.0 were created covering the AOI. Then, density information was extracted at each grid cell by running access\_litho program and providing the latitude and longitude of the respective grid cell. The extracted data at each cell was then arranged in Microsoft excel software for easy processing of the data.

Since the extracted data at each grid cell was composed of several sub layers with different density values, there was a need of computing a weighted density that will represent the overall density of the grid cell. But, the main interest was to acquire the crustal density for computations of terrain correction, therefore only densities of layers above the mean sea level were taken into account. For this case, crust1 (upper crust) sub layer was the layer at which the 0 m depth was found most of the times therefore, density information was computed from crust1 (upper crust) to water sub layer. Weighted density was computed by taking the summation of the product of the density of each sublayer from the crust1 (upper crust) layer and its depth divide by the total depth of all sub-layers.

$$\delta_{wgt} = \frac{\sum(\delta_i \times d_i)}{\sum d_i} \dots\dots\dots (3.4)$$

where,  $\delta_{wgt}$  is the density weight at each extracted grid cell,  $\delta_i$  is the density of the given crustal sub layer and  $d_i$  is the depth of the given crustal sub layer.

Thereafter, the weighted density at each grid cell was gridded in Golden Surfer software by using nearest neighbor gridding method to produce a mass-density model. This model was then used in computations of terrain correction. Figure (3.4) shows an example of density information extracted at grid cell (Pasyanos et al., 2014).

163365.	3300.00	7992.46	4343.73	0.00	70.00	7992.46	4343.73	1.00000	ASTHENO-TOP	
163365.	3300.00	8155.58	4647.05	0.00	200.00	8155.58	4647.05	1.00000	LID-BOTTOM	
47635.	3300.00	8155.58	4647.05	0.00	200.00	8155.58	4647.05	1.00000	LID-TOP	
47635.	3101.90	7341.17	4187.57	0.00	600.00	7341.17	4187.57	1.00000	CRUST3-BOTTOM	
31951.	3101.90	7341.17	4187.57	0.00	600.00	7341.17	4187.57	1.00000	CRUST3-TOP	
31951.	2915.79	6720.79	3867.04	0.00	600.00	6720.79	3867.04	1.00000	CRUST2-BOTTOM	
16259.	2915.79	6720.79	3867.04	0.00	600.00	6720.79	3867.04	1.00000	CRUST2-TOP	
16259.	2812.39	6410.60	3660.25	0.00	600.00	6410.60	3660.25	1.00000	CRUST1-BOTTOM	
94.	2812.39	6410.60	3660.25	0.00	600.00	6410.60	3660.25	1.00000	CRUST1-TOP	
94.	2370.00	4000.00	2130.00	0.00	600.00	4000.00	2130.00	1.00000	SEDS2-BOTTOM	
-57.	2370.00	4000.00	2130.00	0.00	600.00	4000.00	2130.00	1.00000	SEDS2-TOP	
-57.	2110.00	2500.00	1070.00	0.00	600.00	2500.00	1070.00	1.00000	SEDS1-BOTTOM	
-666.	2110.00	2500.00	1070.00	0.00	600.00	2500.00	1070.00	1.00000	SEDS1-TOP	
154892.	3300.00	7988.08	4341.35	0.00	70.00	7988.08	4341.35	1.00000	ASTHENO-TOP	
154892.	3300.00	8151.10	4644.50	0.00	200.00	8151.10	4644.50	1.00000	LID-BOTTOM	

Figure 3.4: Shows sample of the Litho 1.0 crustal density

### 3.2.2 Integration radius

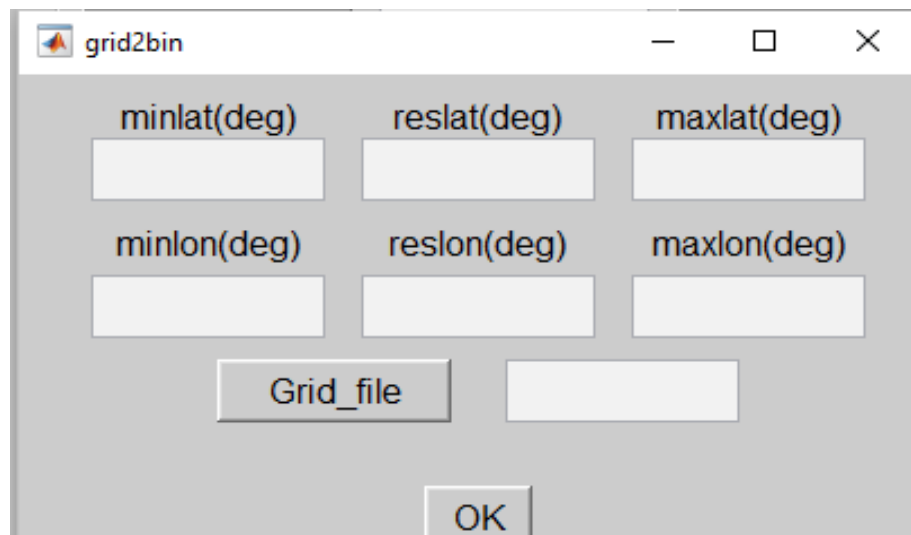
Numerous studies have been performed on the identification and choice of integration radius R1 and R2 based on the required amount of accuracy. Nowell, (1999) outlined different works of literature on the methods for the choice of the integration radiuses. Many authors recommended the value of R1 and R2 to be used. For the choice of R1 values up to 20km and R2 values up to 200km are can be used as a standard. (Hwang et al 2003, Varga et al 2015, Yahaya & Azzab, 2018) recommended that a value Of 20km for R1 and 200km for R2 is sufficient for 0.1mgal precision.

As for this study variation of R was varied up to 10km while keeping the value of R2 constant and obtained the values of the terrain corrections. Again the value of the R1 was kept constant and varied the values of the R2 up 100km. All these variations are referenced from the computation points.

### 3.2.3 Terrain correction computation

The computation was done by using developed MATLAB source code called TGF. This source code receives .bin files of two DEMs of different resolutions and computation points. For this case a downloaded ALOS v3.1-1" was first gridded at 15" and 30" resolutions by using kriging method in golden surfer software, it followed that the two gridded DEMs was then opened in global mapper software for conversion from Geo Tiff (.tiff) format to Gravsoft (. grid) format which is accepted by TGF source code.

Source code consist of interface option of conversion of the grid files to .bin format files accepted for computation of the terrain correction. During conversion of the gridded format DEMs, the maximum and minimum values of latitudes and longitudes are specified as well as resolution of the corresponding DEM. The Figure 3.5 below shows the TGF interface for conversion of gridded file format to .bin format as shown below.

The image shows a MATLAB window titled 'grid2bin'. Inside the window, there are six input fields arranged in a 2x3 grid. The top row fields are labeled 'minlat(deg)', 'reslat(deg)', and 'maxlat(deg)'. The bottom row fields are labeled 'minlon(deg)', 'reslon(deg)', and 'maxlon(deg)'. Below these fields, there is a button labeled 'Grid\_file' and an empty input field. At the bottom center of the window is an 'OK' button. The window has standard MATLAB window controls (minimize, maximize, close) in the top right corner.

*Figure 3.5: Shows the window for the inputs during conversion of grid to binary formats*

After successful conversion of DEMs from gridded format to bin format we had three bin formatted files ready for computation of the terrain corrections. The GUI interface of TGF software in module of forward masses required input file to define the topographic masses, via the geometric upper and lower boundaries and density values. the mass distributions are divided into four zones and defined by three sets of DEM and density inputs, where resolutions varying with zone-distance from computation point. A detailed DEM (pushbuttons— 'DetailedDEM', 'DetailedREF' for RTM computation) defines the masses for polyhedron and prism. 'TessMasses' with 'TESSDEM', 'TESSREF' and 'TessDensity' defines the tesseroid applied zone, and a coarse DEM (pushbuttons— 'CoarseDEM', 'CoarseREF' for RTM computation) are required for point-mass modeling.

In the module 'Gravitational Field', 'ikind' defines the potential type with values of 1 for the topographic gravitational field, and 2 for RTM gravitational field in which for this case of terrain correction computation 1 value have been used. 'itype' defines required computation functions in which option number 4 have been chosen which specifies vertical deflections and gravity anomaly ( $\Delta g$ ). 'rzones' defines the extension of each zone in degree, a prism or polyhedron is suggested in the very near zone (e.g.,  $0.03^\circ$  from calculation point) to avoid unacceptably large errors. For this case value of the r in near zone and far varied so as to obtain different values of the terrain correction which have been used to compute different values of the bouguer gravity anomalies. Figure 3.5 below shows the TGF GUI interface which shows the inputs for the computation of the terrain corrections.

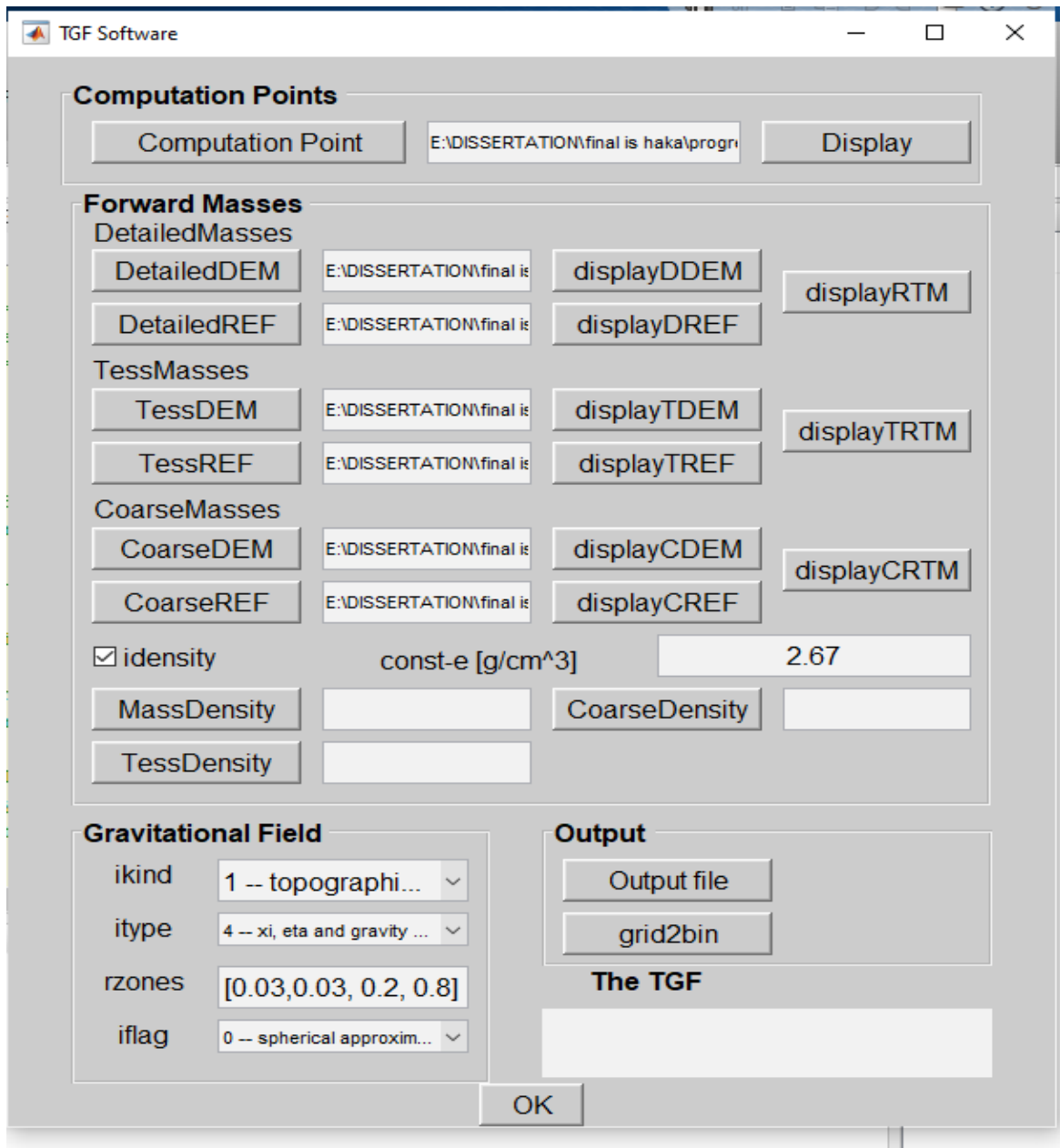


Figure 3.6: Shows the interface of TGF with inputs for computations of terrain correction

After setting all necessary information in TGF GUI interface, the values of the terrain corrections for respective computation points were obtained. Below are the Tables 3.1 & 3.2 of the which shows the summary of the DEMs with their respective resolutions and computation points.



Table 3.1: Distribution of DEMs as used in TGF software in computations of terrain corrections

ZONES	1	2	3	4
NAME	DetailedDEM		TessDEM	CoarseDEM
GEOMETRY	Polyhedron	Prism	Tesseroid	Point-mass
EXTENSION $^{\circ}$ (km)	0.03 (3.24)		0.15 (16.2)	0.8 (86.4)
RESOLUTION (")	15		15	30
FORMAT	.bin		.bin	.bin

Table 3.2: A sample of computation points used in computation of terrain corrections

S/N	Latitude ( $^{\circ}$ )	Longitude ( $^{\circ}$ )	Height (m)
1	-6.986	39.294	76
2	-6.985	39.150	84
3	-6.984	39.532	2
4	-6.980	38.944	251
5	-6.980	38.924	223
6	-6.980	39.520	17
7	-6.974	38.910	206
8	-6.974	39.285	68
9	-6.970	39.154	69

By considering precision based on variation of integration radius and variable crustal density, below are the approach that have been used to compute bouguer gravity anomalies:

- Computation of bouguer gravity anomalies by keeping R1 approximately 3.5km (0.03  $^{\circ}$ ) and outer radius R2 at approximately 90km (0.83 $^{\circ}$ ) i.e. first computation.
- Computation of bouguer gravity anomalies by keeping R2 approximately at 80km (0.74  $^{\circ}$ ) while R1 was kept constant at 3.5km (0.03 $^{\circ}$ ) i.e. second computation.
- Computation of bouguer gravity anomalies by keeping R2 approximately at 90km (0.83 $^{\circ}$ ) while R1 was kept at 5km (0.046 $^{\circ}$ ) i.e. third computation.
- Computation of bouguer gravity anomalies by keeping R2 approximately at 80km (0.74  $^{\circ}$ ) while R1 was kept constant at 5km (0.046 $^{\circ}$ ) i.e. fourth computation.

After obtaining all necessary input data for the computations of the bouguer gravity anomalies which include terrain correction data, phi, lambda, orthometric height H. Bouguer gravity anomalies were computed using MATLAB code developed by (Busega & Kimboi, 2018) with some amendment so as to accommodate the terrain corrections and bouguer attractions. The file that contains data was kept in the same folder as the codes for computations. The code is then run so as the computations started from computing the normal gravity at reference ellipsoid followed by computation of the bouguer attractions and finally bouguer gravity anomalies

### 3.3 Validation of the results

Validation of the results is performed based on the comparison of the statistics between the bouguer gravity anomalies computed by using terrestrial gravity points and relative gravity stations to determine which is the optimum method for creation of that database. By using position i.e. phi and lambda of relative gravity station occupied in my area of the interest (Mussa, 2022), the bouguer gravity anomalies from the computed bouguer gravity anomaly databases were obtained from which they were compared with another computed bouguer gravity anomalies using relative gravity station values.

Table 1.3 Show the statistics used for validations of results

S/N	Statistics	formula
1	Difference between the gravity anomalies; diff	$\Delta g_{relative\ points}^{bou} - \Delta g_{terrestrial\ grav.\ points}^{bou}$
2	Mean; $\bar{X}$	$\frac{\sum diff}{n}$
3	Standard deviation (STD)	$\sqrt{\frac{\sum (X_i - \bar{X})^2}{n - 1}}$
4	Root mean square (RMS)	$\sqrt{\frac{\sum diff^2}{n}}$

### **3.4 Data used**

Below are the data that have been used in this study to achieve the main objective of the research based on the methodology employed:

i. Terrestrial point gravity

The data obtained from Department of Geospatial Sciences and Technology at Ardhi university (DGST). This includes ground and point gravity whereby about 5379 points, 20 relative stations and 1 absolute station over the area of interest (AOI).

ii. Digital elevation model DEMs

ALOS Global Digital Surface Model (ALOS3D30). ALOS v3.1-1" was published on 24th May, 2021 by the Japan Aerospace Exploration Agency (JAXA) was used. It was downloaded freely through the website: <https://www.eorc.jaxa.jp/ALOS/en/aw3d30/data/>. It was used to extract orthometric heights of the required gravity points.

iii. Litho1.0 density model

LITHO1.0 model was downloaded from the official website of the University of California <https://igppweb.ucsd.edu/~gabi/litho1.0.html>. The model was downloaded at its native format and C++ code to read it at any arbitrary location (access\_litho). This data provided information of crustal density distribution at resolution that was used in computations of terrain corrections. It provides the information about the variations of the crustal densities.

### **3.5 Software used**

i. TGF Matlab software

This software was used in computations of terrain corrections using LITHO1.0 crustal density model.

ii. Golden Surfer software (Surfer 15)

The Golden surfer software was used in gridding and preparations of data used in computation of terrain corrections

iii. Global mapper

Global mapper was used in conversion of surfer grid and GeoTiff formats to Gravsoft grid format

iv. Microsoft Excel

Microsoft excel was used in arranging the exported data from LITHO1.0 model and assisted in computation of the weighted density

v. Microsoft word

This software was used in report writing

vi. Generic Mapping Tool (GMT)

The software was used for map drawing of the computed gravity anomalies.

## CHAPTER FOUR

### RESULTS AND DISCUSSION OF THE RESULTS

#### 4.1 Results

In this chapter, the results obtained from the computations of the free-air gravity anomaly and Bouguer gravity anomaly databases will be presented. The research aims to perform various assessments on the obtained results, with a particular focus on the Bouguer gravity anomaly. The objective is to determine, based on these assessments, the most effective method for computing the Bouguer gravity anomaly databases.

##### 4.1.1 Computed normal gravity at reference ellipsoid.

During computation of the gravity anomalies, normal gravity at reference ellipsoid were computed. Below is the Table 4.1 of normal gravity values at GRS80 ellipsoid.

*Table 4.1: Shows values of normal gravity on the reference ellipsoid*

S/N	Latitude	Longitude	Normal gravity at reference ellipsoid ( mGal) .
1	-9.486	39.598	978172.935
2	-9.485	39.470	978172.914
3	-9.473	39.220	978172.554
4	-9.472	39.581	978172.525
5	-9.471	39.468	978172.496
6	-9.471	39.592	978172.490
7	-9.464	39.568	978172.300
8	-9.464	39.599	978172.300
9	-9.486	39.598	978172.935
10	-9.461	39.553	978172.221
11	-9.458	39.491	978172.133
12	-9.457	39.221	978172.101

#### 4.1.2 Computed free-air gravity anomalies

The code developed so as to obtain the values for free-air gravity anomalies from which we can prepare the free-air gravity anomaly database. Table 4.2 below shows sample of computed free-air gravity anomaly.

*Table 4.2: Shows sample of the computed free-air gravity anomaly*

S/N	Latitude	Longitude	Free-air gravity anomalies ( mGal)
1	-9.486	39.598	38.248
2	-9.485	39.470	28.702
3	-9.473	39.220	-8.799
4	-9.472	39.581	33.186
5	-9.471	39.468	27.151
6	-9.471	39.592	24.999
7	-9.464	39.568	29.802
8	-9.464	39.599	9.663
9	-9.486	39.598	22.507
10	-9.462	39.553	37.340
11	-9.459	39.491	7.508
12	-9.458	39.221	38.248
13	-9.456	39.460	25.448
14	-9.454	39.539	28.245
15	-9.450	39.537	27.849

The created grid file for gravity anomaly was used for drawing relief map as shown below in Figure 4.1.

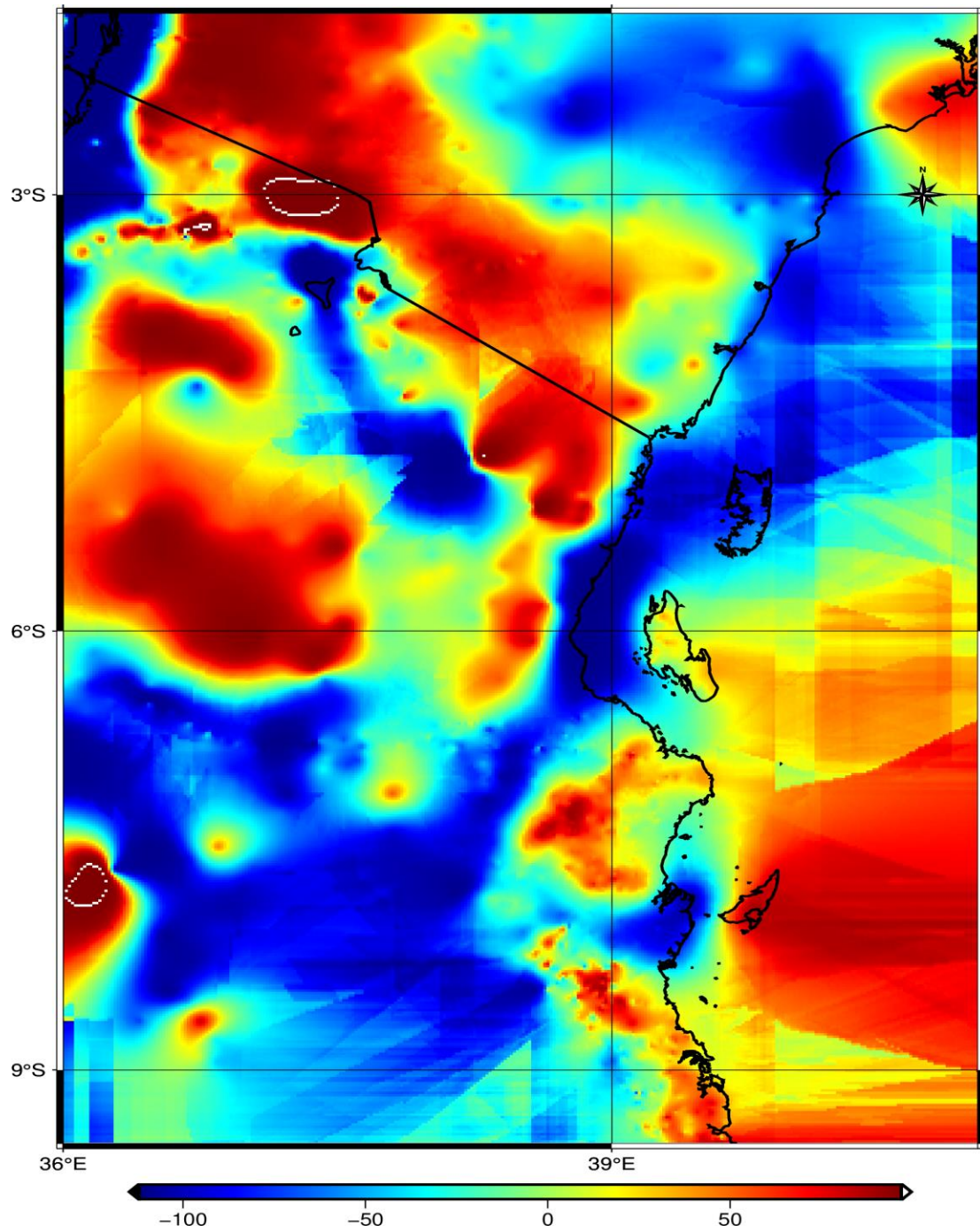


*Figure 4.1: Relief map shows the variation of free-air gravity anomalies*

## 4.2 Bouguer gravity anomaly

Different results obtained during computation of bouguer gravity anomaly. Those values were obtained due to changing of the values of the integration radius during computation of the terrain corrections. In this section the results of bouguer gravity anomaly with the corresponding radii used.

### 4.2.1 First attempt computation of bouguer gravity anomalies

Below is the Table 4.5 of bouguer gravity anomalies when inner radius kept approximately 3.5km and outer radius is approximately 90km.

*Table 4.3 Bouguer gravity anomalies when R1 was kept at approximately 3.5km and R2 at approximately 90km*

S/N	Latitude	Longitude	Bouguer gravity anomalies ( mGal)
1	-9.486	39.598	32.048
2	-9.485	39.470	17.932
3	-9.473	39.220	-40.679
4	-9.472	39.581	26.990
5	-9.471	39.468	16.592
6	-9.471	39.592	19.249
7	-9.464	39.568	24.001
8	-9.464	39.599	4.402
9	-9.486	39.598	17.039
10	-9.461	39.553	29.623
11	-9.458	39.491	-26.490
12	-9.457	39.221	32.048
13	-9.456	39.460	14.358
14	-9.454	39.539	22.986
15	-9.450	39.537	22.571



Below is corresponding relief map of the computed bouguer anomalies.

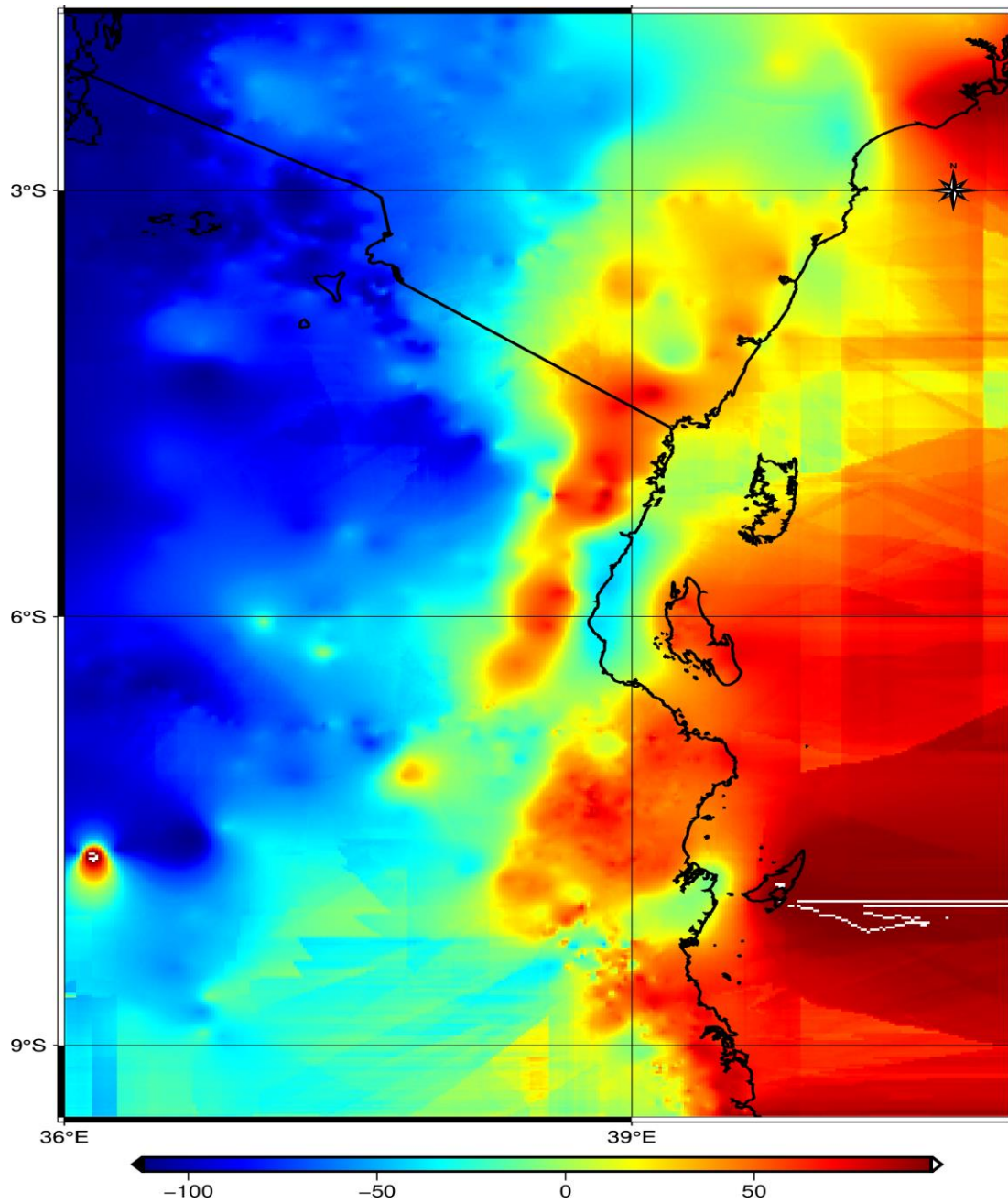


*Figure 4.2: Relief map shows the variation of bouguer gravity anomalies over AOI*

#### 4.2.2 Second attempt computation of bouguer gravity anomalies

Also, bouguer gravity anomaly was computed when R2 is kept approximately at 80km while R1 was kept constant at 3.5km. Below is Table 4.4 of the bouguer gravity anomalies computed

*Table 4.4: Computed gravity anomalies when R2 is kept approximately at 80km while R1 was kept at 3.5km*

S/N	Latitude ( ° )	Longitude ( ° )	Bouguer gravity anomalies ( mGal)
1	-9.486	39.598	-0.984
2	-9.485	39.470	-1.138
3	-9.473	39.220	-61.557
4	-9.472	39.581	-10.530
5	-9.471	39.468	-5.482
6	-9.471	39.592	-12.024
7	-9.464	39.568	-11.887
8	-9.464	39.599	-26.877
9	-9.486	39.598	-7.922
10	-9.461	39.553	-2.684
11	-9.458	39.491	-53.623
12	-9.457	39.221	-0.984
13	-9.456	39.460	-7.934
14	-9.454	39.539	-1.020
15	-9.450	39.537	0.072

Below is the relief map of the computed gravity anomalies drawn by using GMT

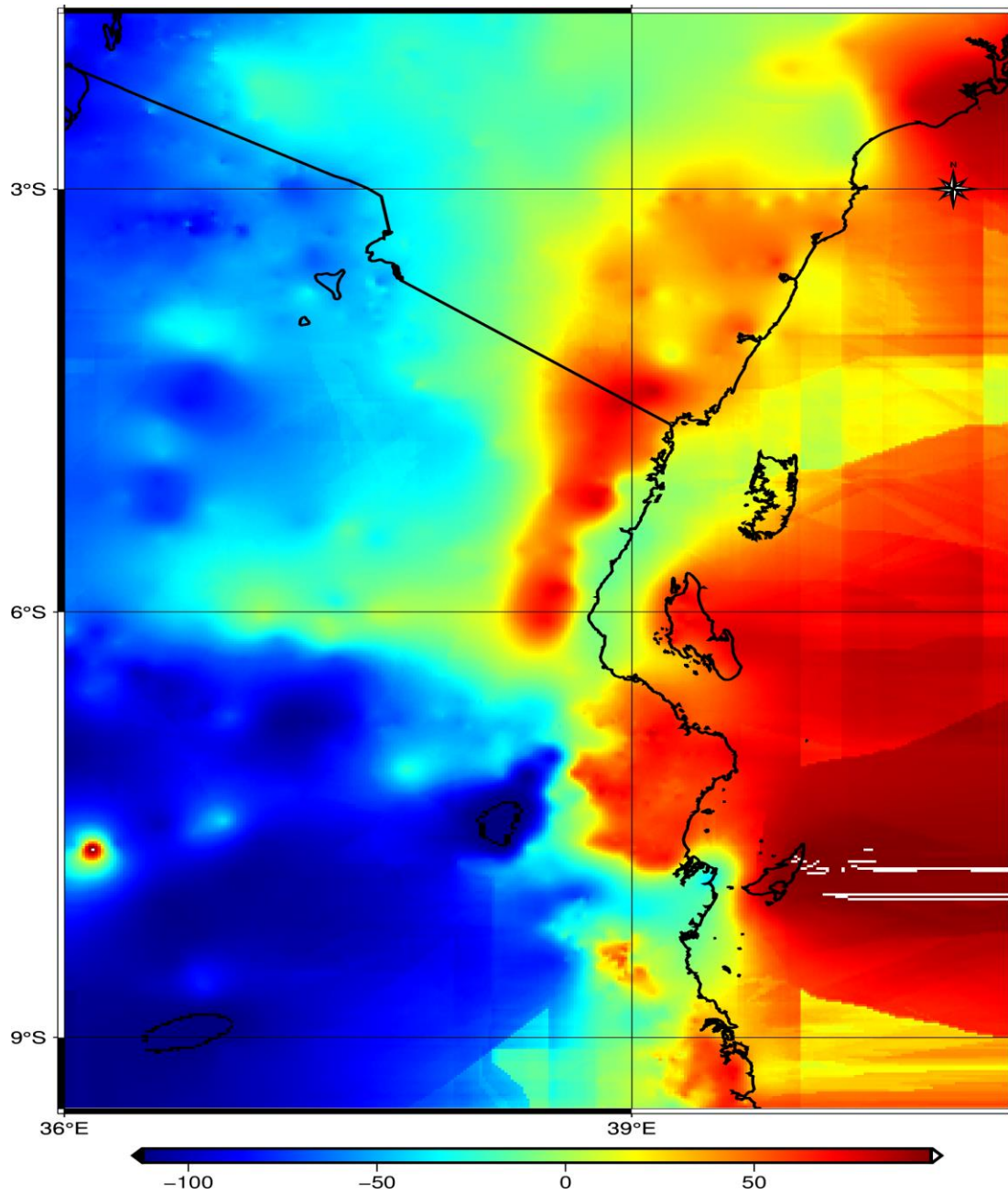


*Figure 4.3: Shows the variation of second computed bouguer gravity anomalies*

### 4.2.3 Third attempt computation of bouguer gravity anomalies.

Another computation of bouguer gravity anomaly was computed when R2 is kept approximately at 90km while R1 was kept constant at 5km. Below is the table of values of the bouguer gravity anomalies computed.

*Table 4.5: R2 is kept approximately at 90km while R1 was kept constant at 5km*

S/N	Latitude	Longitude	Bouguer gravity anomalies ( mGal)
1	-9.486	39.598	1.789
2	-9.485	39.470	-3.147
3	-9.473	39.220	-142.493
4	-9.472	39.581	-13.141
5	-9.471	39.468	-9.986
6	-9.471	39.592	-1.532
7	-9.464	39.568	-11.472
8	-9.464	39.599	-11.795
9	-9.461	39.553	7.530
10	-9.458	39.491	-11.295
11	-9.457	39.221	-152.792
12	-9.486	39.598	1.789
13	-9.456	39.460	-13.292
14	-9.454	39.539	15.460
15	-9.450	39.537	17.793

Below is the relief map of the computed gravity anomalies drawn by using GMT.

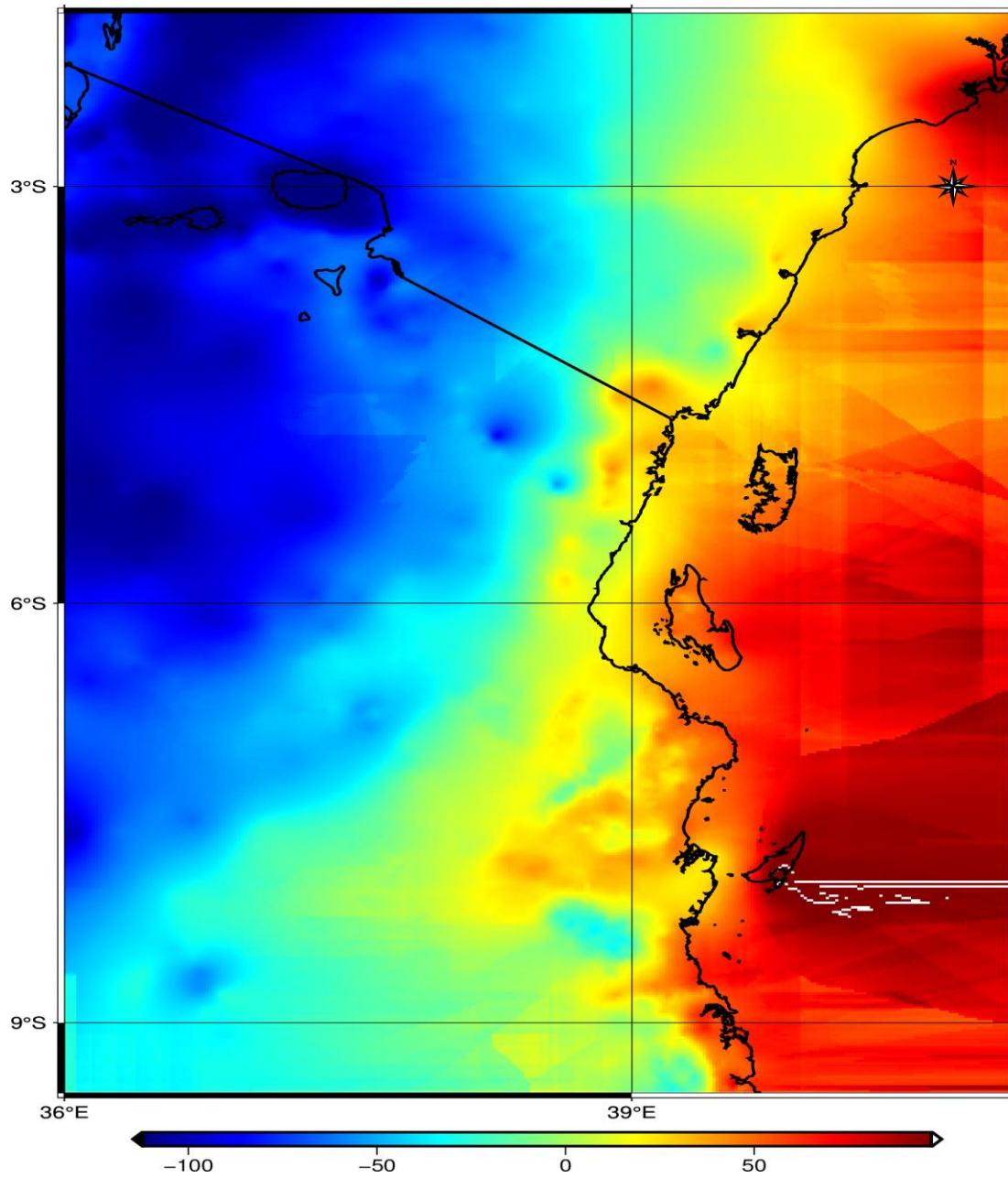


*Figure 4.4: Relief map shows variation of the third computed bouguer gravity anomalies*

#### 4.2.4 Fourth attempt computation of bouguer gravity anomalies.

Final computation of bouguer gravity anomaly was computed when R2 is kept approximately at 80km while R1 was kept constant at 5km. Below is the table of values of the bouguer gravity anomalies computed.

*Table 4.6: R2 is kept approximately at 80km while R1 was kept constant at 5km*

S/N	Latitude	Longitude	Bouguer gravity anomalies ( mGal)
1	-9.486	39.598	-31.243
2	-9.485	39.470	-22.218
3	-9.473	39.220	-163.371
4	-9.472	39.581	-50.662
5	-9.471	39.468	-32.060
6	-9.471	39.592	-32.805
7	-9.464	39.568	-47.360
8	-9.464	39.599	-43.075
9	-9.461	39.553	-17.431
10	-9.458	39.491	-43.602
11	-9.457	39.221	-179.925
12	-9.486	39.598	-31.243
13	-9.456	39.460	-35.584
14	-9.454	39.539	-8.545
15	-9.450	39.537	-4.705



Below is the relief map drawn by using GMT over the AOI.

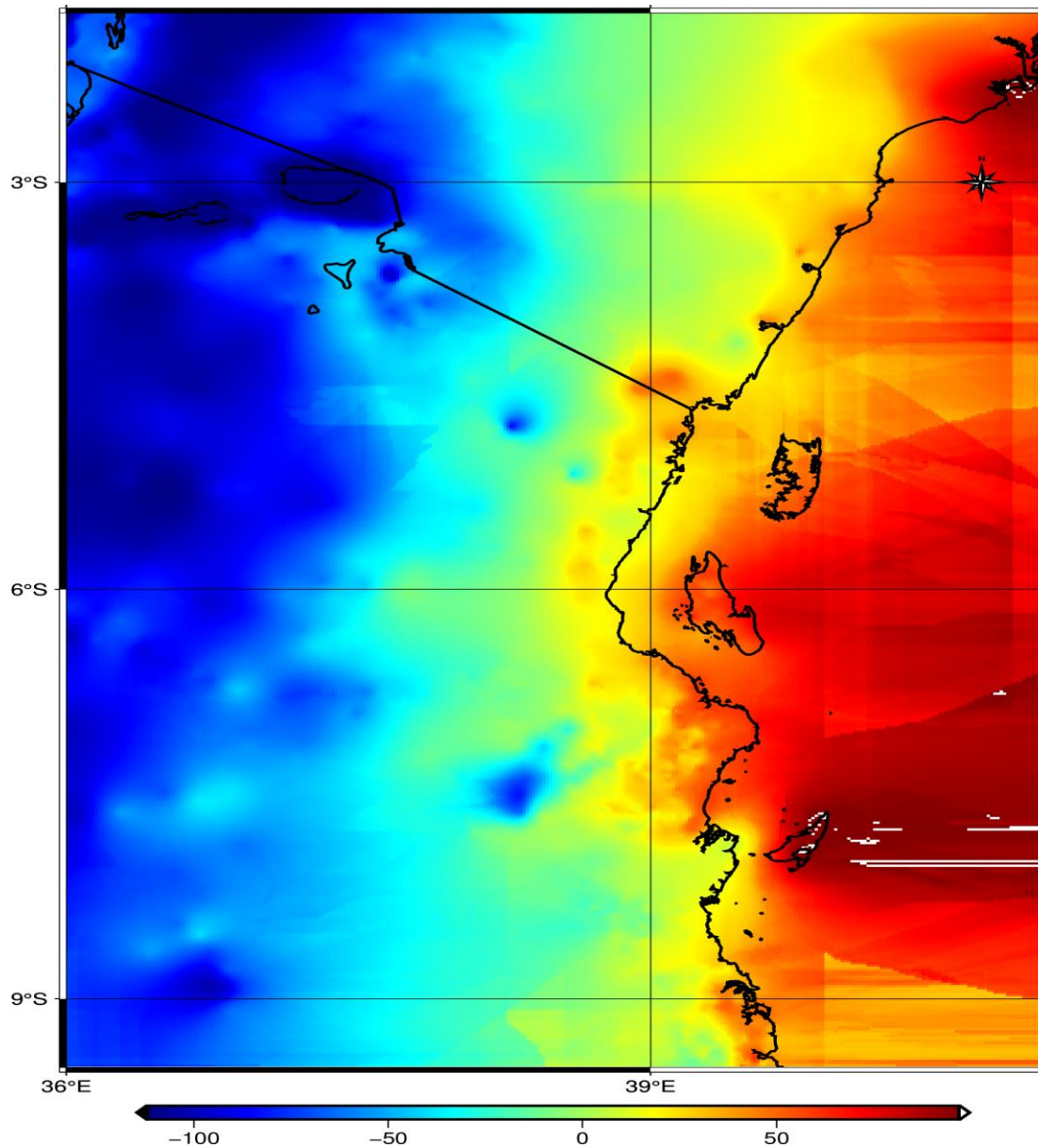


*Figure 4.5: Relief map showing the variation of computed bouguer gravity anomalies*

After computation of the bouguer gravity anomalies as well as free-air gravity anomalies, the best result which represented the optimal method for creation of free-air and bouguer gravity anomaly were used to create databases i.e. surfer grid file.

### 4.3 Quality check

Quality assessment of the results was done by comparing computed gravity anomalies by using terrestrial points gravity with the gravity anomalies computed by using the relative gravity stations, the difference, mean and standard deviation between gravity anomalies computed using terrestrial gravity station and those computed using relative gravity stations was observed. 15 relative station out of 56 relative station was used. Table 4.7 below shows minimum, maximum, mean, standard deviation as well root mean square of the difference between the two computed anomalies.

*Table 4.7: Shows the validation results of bouguer anomalies*

S/N	Bouguer computation	Minimum value	Maximum value	Mean	STD	RMS
1	First comp	-21.233	3.381	-9.167	8.329	11.922
2	Second comp	-21.249	1.590	-9.290	8.000	12.161
3	Third comp	-3.610	9.961	1.398	3.752	3.884
4	Fourth comp	-3.599	8.236	1.044	3.189	3.849

For the case of free-air gravity anomalies, the results of the difference between free-air gravity anomaly computed using terrestrial gravity points and those of the relative gravity points were tabulated as:

*Table 4.8: Shows the validation of free-air anomalies*

Gravity anomaly	Minimum	Maximum	Mean	STD	RMS
$\Delta g_{FA}$	-6.345	8.164	-0.966	4.133	4.109

#### 4.3.1 Discussion of the results

From the aforementioned results obtained from the series of computations of the Bouguer gravity anomalies, notable differences were observed in the STD and RMS values among the computations. These variations were attributed to the variation in the integration radius used in the computation points as well as used variable density LITHO1.0. Notably, the fourth method emerged as the optimal approach for creating the classical Bouguer gravity anomaly, as it yielded the lowest STD and RMS values compared to the other three methods.



Additionally, in the case of the free-air gravity anomaly, the approach that considered elevation proved to be optimal, resulting in smaller STD and RMS values. This suggests that considering elevation in the computation process led to more accurate and reliable results for the free-air gravity anomaly.

These findings highlight the importance of carefully selecting the appropriate methods and parameters for computing both Bouguer and free-air gravity anomalies to ensure the accuracy and reliability of the results.

## **CHAPTER FIVE**

### **CONCLUSION AND RECOMMENDATIONS**

#### **5.1 Conclusion**

The main objective of this dissertation have been fulfilled since optimal method for creation of classical bouguer have been determined as well as for the case of the free-air gravity anomaly. Different results were obtained based on the method used from which validation have been done so as to determine which one is optimal.

From those anomalies computed over the AOI, one of the smallest root mean square and standard deviation which were 3.849mgal and 3.189mgal respectively was referred as the optimal method for the creation of the classical bouguer which were obtained by keeping inner integration radius R1 5km (0.046°) and outer integration radius R2 80km (0.74 °). For the case of the free-air gravity anomalies root mean square obtained were 4.109mgal and standard deviation of 4.133mgal was referred as the optimal for creation of corresponding database. These methods can be used for creation of databases which can be used for various purposes like identifying potential hazards, mineral explorations and infrastructure planning.

#### **5.2 Recommendation**

1. Due to the daily improve of the technology and updating of the data, effort should have to done periodically to update these databases so as to obtain most accurate information for various daily uses. Updating of DEMs will result more accurate topographic corrections which will lead to more accurate databases.
2. It is recommended that researchers explore and consider alternative variable density models and compare the terrain corrections obtained using LITHO1.0 with those derived from the other density model. This comparison would provide valuable insights into the impact of different density models on the accuracy and reliability of the terrain corrections

## References

- Abadalla, A. A. (2009). *Determination of a Gravimetric Geoid Model of Sudan Using the KTH*. Stockholm Sweden: Master's of Science Thesis in Geodesy, Division of Geodesy, School of Arch. & Built Env. KTH.
- Amante, C., & Eakins, B. (2009). *ETOPO1 1 arc-minute Global Relief model: Procedures*. NOAA Technical Memorandum NESDIS NGDC, 19.
- Busega, H., & Kimboi, M. (2018). Surface gravity anomaly database for gravimetric geoid model computation of Tanzania using KTH method. *A B.Sc. Dissertation of the department of Geospatial Sciences and Technology. Dar-es-Salaam Tanzania: Ardhi University*.
- Hinze, W. (2003). *Bouguer reduction density, why 2.67*. Geophysics 68(5), 1559–1560.
- Hoffman-Wellenhof, B., & Moritz, B. (2005). *Physical Geodesy (1st ed.)*. New York, USA: Technische Univesitat.
- Laske, G., Masters, G., & Pasyanos, M. (2013). *CRUST1.0: A New Global Crustal at 1x1 degree*. Retrieved July 24, 2020.
- Mussa, I. H. (2022). 1'x1' full spectrum surface gravity anomaly for Zanzibar. *A B.Sc. Dissertation of the department of Geospatial Sciences and Technology. Dar-es-Salaam Tanzania: Ardhi University*.
- Nchambi, N. L. (2021). Determination of Tanzania gravity database of 021(TGDB21). *A B.Sc. Dissertation of the department of Geospatial Sciences and Technology. Dar-es-Salaam Tanzania: Ardhi University*.
- Nowell, A. D. (1999). *Gravity terrain corrections—an overview*. 41(3), 231-246: Journal of Applied Geophysics,.
- Pasyanos, M., Masters, G., Laske, G., & Ma, Z. (2014). *LITHO1.0: An Updated Crust and Lithosphere Model of the Earth*. *J. Geophyscis Res. Solid Earth*. 119, 2153-2173.
- Peter, R. V. (2018). Tanzania Gravimetric Geoid Model (TZG17) through Quasi-Geoid by The KTH Method. *A M.Sc. Dissertation of the Department of Geospatial Sciences and Technology. Dares-Salaam Tanzania: Ardhi University*.

- Petr, V., & Edward, J. (1986). *Geodesy: The concept*. North-Holland: Elsevier science publishers B.V., 1986.
- Tenzer, R., Sirguey, P., Rattenbury, M., & Nicolso. (2011). *A digital rock density map of New Zealand*. Computers & Geosciences, 37, 1181-1191.
- Ulotu, P. E. (2016). *Integration of Tanzania New Gravity Network and Database into Vertical* . International Journal of Engineering Science and Computing.
- Vanicek, P. (1986). *Geodesy: The concepts* (Vol. Second edition). North-Hollarnd, Netherlnds: Elsevier Science Publishers B.V.
- Varga M, Grgić M, Oršulić OB & Bašić T. (2019). *Influence of digital elevation model*. Croatia: Geofizika, 36(1),.
- Vermeer, M. (2020). *Physical geodesy, (2nd ed., pp. 45-68)*. Helsinki, Finland: Aalto University publication series science + technology.
- Yahaya SI & Azzab DE. (2008). *High-Resolution Residual Terrain Model and Terrain* . Zger Republic.: Geodesy and Cartography, 44(3), 89.

## APPENDICES

Appendix 1: Matlab code for computation of free-air gravity anomalies and bouguer gravity anomalies.

```

1  % Program name :
2  % Point gravity 2 free-air gravity anomaly and bouguer gravity anomaly
3  %
4  % Description :
5  % This program computes free-air gravity anomaly and bouguer gravity
6  % anomaly from point
7  % gravity on surface of the earth .
8  %
9  % Normal gravity gamma_GRS80 is based on GRS80 reference ellipsoid .
10 % Gravity is in mGal units .
11 %
12 % Input :
13 % 1. Station file containing the point gravity . The input
14 % file should not contain header info but have columns
15 % arranged in the form : phi lambda H g( mGal ) and terrain corrections (
16 mgal)
17 %
18 % NB: The station file should be named " input.txt" or it should
19 % be changed before executing the program
20
21 % Programmer : ABDUL-RAHIM MUHIJA JUMA
22 % Created : 2023
23 %-----
24 load input_05.txt;
25 mat = input_05;
26 phi = mat (: ,1) ; % latitude
27 lambda = mat (: ,2) ; % longitude
28 H = mat (: ,3) ; % Orthometric height
29 g = mat (: ,4) ; % Point gravity ( mGal )
30 t = mat (: ,5) ; %terrain correction
31
32 % -----
33 % Computation of normal gravity ( gamma_grs ) referred to GRS80
34 % Units in mgal
35 % -----
36 gamma_GRS80 = 978032.67715*(1+0.0052790414*( sind ( phi ) .^2) +...
37 0.0000232718*( sind ( phi ) .^4) ...
38 + 0.0000001262*( sind ( phi ) .^6) +0.0000000007*( sind ( phi ) .^8) ) ;
39
40 % -----
41 % Computation of Free Air Gravity Anomalies ( delta_g_air )
42 % Units in mgal
43 % -----
44 delta_g_air = g + 0.3086* H - gamma_GRS80 ;
45
46 %-----
47 % Computation of bouguer gravity anomaly ( delta_g_bou ) i.e refine bouguer
48 % gravity anomaly since it include terrain correction
49 % Units mgal
50 %-----
51 delta_g_bo = g - 0.3086*H + 0.1119* H + t - gamma_GRS80 ;

```

## Appendix 2: GMT code for gravity anomalies drawings over the AOI

```
1  gmt begin 1 png
2  set FONT Times-BoldItalic
3  REM Set variables for all grids
4  set cpt1=rte1.cpt
5  set cpt2=rte2.cpt
6  set grd1=g_anomalies.grd
7  set grd2=rte1.nc
8
9  REM Make CPT for visualizing the RTE grid
10 gmt makecpt -Cjet -T0/255/1 -H -Z > %cpt1%
11 gmt makecpt -Cjet -T-112/97 -H -Z > %cpt2%
12
13 REM Histogram Equalize the input grid
14 gmt grdhisteq %grd1% -G%grd2% -C256
15
16 REM Convert the Histogram Equalized grid above to image
17 gmt grdimage %grd2% -C%cpt1% -JM6i -R36/43/-9.5/-1.75 -Ba3g3
18
19 REM Map border & Frame
20 gmt basemap -JM6i -Ba3g3 -R36/43/-9.5/-1.75
21
22 REM Map Coastlines
23 gmt coast -Dh -N1/1.35p -W1.25p -R36/43/-9.5/-1.75 -Tdg39.5.0/-
24 1.5+w1.0c+f2+l,,N
25
26 REM Add Color Legend
27 gmt colorbar -DJBC+w5i/0.12i+h+e -C%cpt2% -Ba
28
29 REM Delete un-neccesary files
30 Del *.nc *.cpt
gmt end
```







